

LIBRARY

LIBRARY

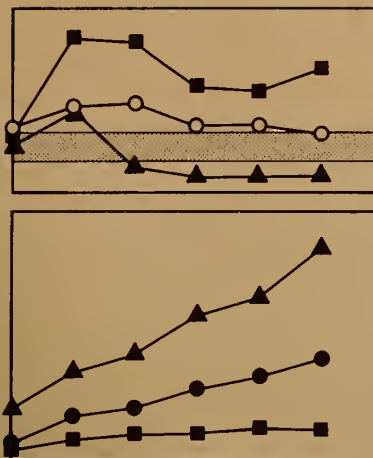
JUN 12 1997

IL GEOL SURVEY

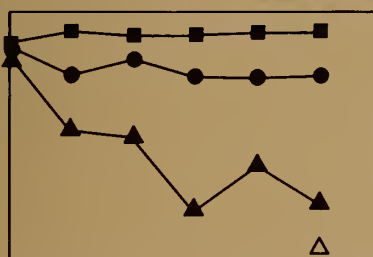
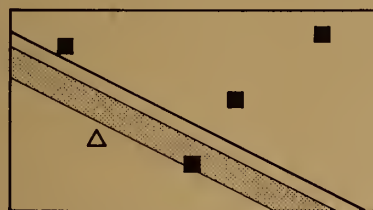


S  
14. GS:  
EGN 130  
c.1

*Geol Survey*



# Geochemical interactions of hazardous wastes with geological formations in deep-well systems

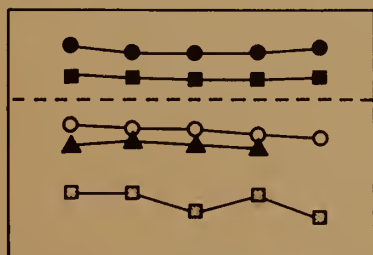


W. R. Roy  
S. C. Mravik  
I. G. Krapac  
D. R. Dickerson  
R. A. Griffin



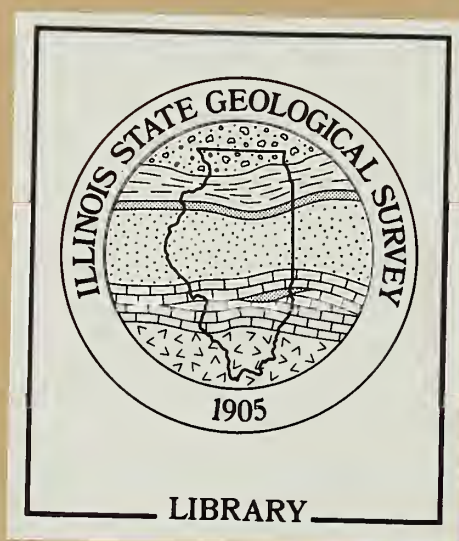
Department of Energy and Natural Resources  
ILLINOIS STATE GEOLOGICAL SURVEY

ENVIRONMENTAL GEOLOGY NOTES 130 1989



APR 19 1989  
ILLINOIS STATE  
GEOLOGICAL SURVEY  
LIBRARY

This report was prepared for the Office of Drinking Water, WH 550, U.S. Environmental Protection Agency, 401 M Street SW, Washington, DC 20460, Cooperative Agreement CR 813-147-01, and Hazardous Waste Research and Information Center, 1808 Woodfield Drive, Savoy, Illinois 61820, HWRIC Project Number HWR 86015.



*Editor: Joan M. Stolz*  
*Graphic Artist: Peter M. Ryan*

---

Roy, W. R. (William R.)

Geochemical interactions of hazardous wastes with geological formations in deep-well systems / W. R. Roy . . . et al. — Champaign, IL: Illinois State Geological Survey, 1989.  
vii, 52 p.; 28 cm. — (Environmental geology notes; 130)

1. Geochemistry. 2. Hazardous wastes—Disposal. 3. Waste disposal in the ground—Illinois. 4. Injection wells. I. Title. II. Series.

---

*Printed by authority of the State of Illinois / 1989 / 750*

ILLINOIS STATE GEOLOGICAL SURVEY



3 3051 00005 4845

# **Geochemical interactions of hazardous wastes with geological formations in deep-well systems**


**W. R. Roy  
S. C. Mravik  
I. G. Krapac  
D. R. Dickerson  
R. A. Griffin**

ILLINOIS STATE  
GEOLOGICAL SURVEY  
LIBRARY  
APR 19 1989

**ENVIRONMENTAL GEOLOGY NOTES 130 1989**

**ILLINOIS STATE GEOLOGICAL SURVEY  
Morris W. Leighton, Chief**

**Natural Resources Building  
615 East Peabody Drive  
Champaign, Illinois 61820**



Digitized by the Internet Archive  
in 2012 with funding from  
University of Illinois Urbana-Champaign

<http://archive.org/details/geochemicalinter130royw>



## **CONTENTS**

ACKNOWLEDGMENTS vi

ABSTRACT vii

EXECUTIVE SUMMARY viii

INTRODUCTION 1

EXPERIMENTAL OBJECTIVES AND APPROACH 3

ANALYTICAL METHODS 4

Characterization of the Core Samples 6

Chemical Characterization of the Acidic Waste 8

Chemical Characterization of the Alkaline Waste 8

Chemical Characterization of the Connate Formation Brine 12

RESULTS 14

Acidic Waste-Rock Interactions 14

Alkaline Waste-Rock Interactions 23

CONCLUSIONS 31

Waste Interactions with the Mt. Simon Sandstone 31

Waste Interactions with the Potosi Dolomite 32

Waste Interactions with the Proviso Siltstone 33

REFERENCES 35

APPENDIX A Glossary 38

APPENDIX B Laboratory Procedure for Conducting Batch Interaction Studies 39

APPENDIX C Geologic Descriptions of Core Intervals Sampled for this Project 44

APPENDIX D Application of Ion Chromatography to Derive Oxidation-Reduction Potentials 49

## TABLES

1	Quality assurance-quality control standards used in this project	4
2	Detection limits, percent bias, and coefficient of variation for each constituent and the variance associated with the samples	5
3	Particle-size data for the three disaggregated core samples	8
4	Chemical composition of the acidic waste sample	9
5	Inorganic chemical composition of the alkaline waste sample	10
6	Gas chromatographic-mass spectrometric analysis of the base-neutral fraction of the alkaline waste	11
7	Gas chromatographic-mass spectrometric analysis of the acid fraction of the alkaline waste	12
8	Gas chromatographic analysis of the alkaline waste: volatile organic compound detected	12
9	Chemical composition of formation brine samples collected from the Velsicol observation well	13
10	Mean concentration of percent CO <sub>2</sub> in gas samples	18
11	Calorimetric determinations of heats of reaction between the acidic waste and the core samples	20
B1	Composition of the pressure vessels and the occurrence of solute artifacts	41
C1	Description of the Potosi Dolomite	44
C2	Description of the Proviso Siltstone of the Eau Claire Formation	46
C3	Description of the Mt. Simon Sandstone	48
D1	Oxidation-reduction potential measurements as a function of time	49

## FIGURES

1	Stratigraphic relationships between the Potosi Dolomite, Eau Claire Formation, and Mt. Simon Sandstone from northwestern to southeastern Illinois	7
2	Change in solution pH of the acidic waste when mixed with the Mt. Simon Sandstone in a closed and low-oxygen system as a function of time, temperature, and pressure	14
3	Change in solution pH of the acidic waste when mixed with the Potosi Dolomite	15
4	Change in the oxidation-reduction potential of the acidic waste when mixed with the Proviso Siltstone	15
5	Concentration of calcium in the acidic waste and waste-brine mixture after 15 days of contact with the Mt. Simon Sandstone, Potosi Dolomite, and Proviso Siltstone	16
6	Change in solution concentration of calcium in the acidic waste when mixed with the Proviso Siltstone	17
7	Change in solution concentration of magnesium in the acidic waste when mixed with the Potosi Dolomite	17
8	Concentration of aluminum in the acidic waste after 15 days of contact with the Mt. Simon Sandstone, Potosi Dolomite, and Proviso Siltstone	19
9	Solution concentration of silica in the acidic waste and the waste-brine mixture when mixed with the Mt. Simon Sandstone	19
10	Silica equilibria of the unreacted acidic waste, waste-Mt. Simon Sandstone mixtures, and the waste-brine-sandstone system after 15 days of solid-liquid contact	21
11	Silica equilibria of the unreacted acidic waste, waste-Potosi Dolomite mixtures, and the waste-brine-dolomite system after 15 days of solid-liquid contact	22
12	Oxidation-reduction potential of the alkaline waste when mixed with the Proviso Siltstone	24
13	Solution concentration of calcium in the alkaline waste when mixed with the Potosi Dolomite	24
14	Concentration of calcium in the alkaline waste and the waste-brine mixture after 15 days of contact with the Mt. Simon Sandstone, Potosi Dolomite, and Proviso Siltstone	25
15	Solution concentration of sulfate in the alkaline waste and the waste-brine mixture when mixed with the Mt. Simon Sandstone	26
16	Solution concentration of silica in the alkaline waste and the waste-brine mixture when mixed with the Mt. Simon Sandstone	26
17	Solution concentration of silica in the alkaline waste and the waste-brine mixture when mixed with the Proviso Siltstone	27

- 18 Concentration of silica in the alkaline waste and waste-brine mixture after 15 days of contact with the Mt. Simon Sandstone, Potosi Dolomite, and Proviso Siltstone 27
- 19 Solution concentration of aluminum in the alkaline waste after 15 days of contact with the Mt. Simon Sandstone 28
- 20 Calcite equilibria of the alkaline waste-Mt. Simon Sandstone mixtures and the waste-brine-sandstone system after 15 days of solid-liquid contact 29
- 21 Calcite equilibria of the alkaline waste-Potosi Dolomite mixtures and the waste-brine-dolomite system after 15 days of solid-liquid contact 30
- B1 Parr pressure vessel with modifications 40
- B2 Solution iron concentration in the acidic waste when mixed with the Mt. Simon Sandstone at 298°K-0.1 MPa in Hastelloy pressure vessels and in Nalgene plastic bottles 41
- D1 Distribution of oxidation-reduction potentials as a function of time for the Mt. Simon-acidic waste mixture derived by ion chromatography, dichromate titration, and platinum electrode 51
- D2 Agreement between  $\text{Fe}^{2+}$  determinations derived from dichromate titration and ion chromatography 51

## **ACKNOWLEDGMENTS**

The authors gratefully acknowledge the partial support of this project by the U.S. Environmental Protection Agency, Office of Drinking Water, Washington, D.C. David Morganwalp was the project officer of Cooperative Agreement CR-813-147-01. This project was also supported by the Hazardous Waste Research and Information Center of Illinois. Gary D. Miller was the project officer of Illinois Department of Energy and Natural Resources Grant No. HWR 86015.

The collection of the hazardous waste and brine samples from the Velsicol Chemical Corporation was facilitated by Jeffrey S. Brown who also provided technical data on the composition of the waste--we thank him for his cooperation and advice. The hazardous waste was collected from the Cabot Corporation, Tuscola, Illinois, with the cooperation with Larry L. Crews.

Thomas C. Buschbach, Illinois State Geological Survey (ISGS) Emeritus, assisted with core descriptions and sampling to ensure that the samples collected were representative of the formations. Ross D. Brower and Edward Mehnert of the ISGS provided technical assistance, particularly in the collection of the brine sample, and background data on the Velsicol site. Randall E. Hughes and Robin L. Warren conducted all of the mineralogical characterizations, which were crucial to this project. S.F. Joseph Chou prepared the Velsicol sample for the characterizations by gas chromatography-mass spectroscopy. We also thank Robert R. Frost and Michael L. Sargent of the ISGS for analytical services and drill core information, respectively. Rebecca J. Roeper provided the particle-size data for the core samples. Michael R. Schock of the Illinois State Water Survey made available a ferrous iron automated titrator and the thermodynamic model SOLMNEQF. We also thank the three anonymous reviewers who critically evaluated this report.



## ABSTRACT

Geochemical interactions of two liquid hazardous wastes with geologic materials from deep-well injection zones in Illinois were investigated by conducting laboratory studies. The liquid wastes included a dilute inorganic acid and a concentrated alkaline brine-like solution. The wastes were mixed with disaggregated core samples of two injection formations, the Mt. Simon Sandstone and Potosi Dolomite. Interactions were also studied with the Proviso Siltstone, which is considered part of a confining layer at two deep-well facilities in Illinois.

The core samples were mixed with each of the liquid wastes for 15 days. These batch-mixing experiments were conducted under low-oxygen conditions in pressure vessels that were simultaneously heated and pressurized to simulate subsurface conditions at three temperatures and pressures (298°K-0.1 MPa, 313°K-6.0 MPa, and 328°K-11.7 MPa). Additional experiments were conducted by diluting the wastes (1:1, vol/vol) with a connate formation brine to simulate the mixing zone in an injection scenario. The gas and liquid phases were analyzed to determine reaction products. Thermodynamic modeling, coupled with mineralogical data, was applied to derive reaction mechanisms.

The acidic waste was neutralized when reacted with the dolomite and siltstone via carbonate dissolution with the concomitant generation of dissolved carbonate species and carbon dioxide. The acidic waste was partially neutralized by the sandstone via the dissolution of clay minerals and ion exchange, augmented by the dissolution of a small amount of dolomitic material. With pH used as the hazardous criterion, the alkaline waste remained hazardous after reacting with the formation samples at 298°K-0.1 MPa and 313°K-6.0 MPa. At 328°K-11.7 MPa, the waste-formation mixtures were not hazardous by definition, but remained highly alkaline. The silica solid phases of the Mt. Simon Sandstone and Proviso Siltstone dissolved in the alkaline waste. The Potosi Dolomite was the least reactive of the three formations. In some cases, solution equilibria could be modeled using the thermodynamic principles of dissolution-precipitation of mineral phases. In other cases, empirical laboratory-based investigations are needed to assess the chemical interactions between injected wastes, injection formations, and associated formation waters.

## EXECUTIVE SUMMARY

This laboratory study was undertaken to develop basic geochemical data that would lead to a more complete understanding of inorganic reactions between two liquid hazardous wastes and three subsurface injection formations. Two liquid waste samples were collected and analyzed: 1) a dilute inorganic acidic solution (pH 1.9) that was a by-product of the production of amorphous silica by the Cabot Corporation, and 2) an alkaline brine-like solution (pH 12.8) that was a caustic process water from the synthesis of pesticides by the Velsicol Corporation. Both waste liquids are currently injected into deep wells in Illinois. The injection-zone materials studied included the Mt. Simon Sandstone and Potosi Dolomite, two formations that are used for waste disposal in Illinois. The Proviso Siltstone of the Eau Claire Formation was also included in this study as a material representative of the confining layer in deep-well scenarios. The Eau Claire Formation overlies the Mt. Simon Sandstone. A connate formation brine sample was included in some of the studies to simulate the mixing zone near the injection well.

The waste-rock interactions were investigated by conducting 15-day batch-mixing studies. These studies were conducted under low-oxygen conditions in pressure vessels that were simultaneously heated and pressurized to simulate subsurface conditions. Temperatures and pressures corresponding to three depths of injection were used in this investigation: 298°K-0.1 MPa (surface), 313°K-6.0 MPa (depth, 457 m), and 328°K-11.7 MPa (depth, 914 m). Disaggregated core samples of each formation were mixed with the liquids using a 1:4 solid-to-liquid ratio (wt/vol). The formation brine was used only in the 328°K-11.7 MPa studies. Each waste was diluted with the connate formation brine as a 1:1 (vol/vol) mixture.

Under the laboratory conditions described, the acidic waste was either partially or entirely neutralized when mixed with each of the three formation samples. In the case of the Mt. Simon Sandstone, the pH of the solution increased, via the dissolution of clay minerals and ion exchange, augmented by the dissolution of a minor amount of dolomitic material. The pH of the solution increased slightly with an increase in temperature and pressure. The pH of the acidic waste was between 6.5 and 7.4 after 15 days of contact with either the dolomite or the siltstone. The distribution of pH values did not correlate with the temperature and pressure of the system. The neutralization mechanism was the dissolution of carbonates with the concomitant generation of carbonate species and carbon dioxide. The solutions were apparently undersaturated with respect to CO<sub>2</sub> because significant exsolution of a gas phase was not detected in gas samples collected at the elevated pressures.

The thermodynamic computer models WATEQ2 and SOLMNEQF were applied to help determine solution equilibria. The acidic waste-Mt. Simon system appeared to equilibrate with chalcedony at each temperature and pressure, and thus silica dissolution could be predicted over the temperature-pressure range studied. Carbonate equilibrium was not established. Both the acidic waste-dolomite and waste-siltstone systems were supersaturated with respect to dolomite and calcite. The acidic waste-dolomite mixtures did not equilibrate with a SiO<sub>2</sub>-solid phase, whereas the activity of silica in the waste-siltstone system appeared to be influenced by the solubility of chalcedony.

With pH as the hazardous-waste criterion, the brine-like alkaline waste remained hazardous after contact with the three core materials at 298°K-0.1 MPa and 313°K-6.0 MPa. The pH values of the solution phases remained above 12.5. At 328°K-11.7 MPa, the pH values were less than 12.5, but the solutions remained highly alkaline, ranging in pH from 11.5 to 12.4. In the three systems studied, only minor gaseous evolution of carbon dioxide was detected at atmospheric pressure. At the elevated pressures, no exsolution of a gas phase was detected.

When the alkaline waste was mixed with a connate formation brine, carbonate phases and possibly magnesium hydroxide precipitated under all temperature and pressure conditions. The alkaline waste contained an excess of CO<sub>3</sub><sup>2-</sup>, which readily precipitated with divalent metals. In an unrelated study, brucite (Mg(OH)<sub>2</sub>) was detected near the injection zone at the Velsicol plant.



Chemical interactions between the inorganic acidic waste and the core samples were mostly carbonate reactions. Interactions associated with the highly alkaline waste were primarily related to the dissolution of silicates. On the basis of the amount of silica found in solution, approximately 0.2 percent of the sandstone dissolved after 15 days of contact with the alkaline liquid waste at 328°K-11.7 MPa. However, the dissolution of silica could not be described by the thermodynamic solubility of any solid  $\text{SiO}_2$  phase, possibly due to nonequilibrium conditions or mixed-phase solids.

The Potosi Dolomite was only sparingly soluble in terms of silica dissolution, whereas the amount of silica in solution from the Proviso Siltstone translated to approximately 0.3 percent dissolution of the solid mass after 15 days of exposure to the alkaline waste. It appeared that the physical integrity of the siltstone would be more challenged by a highly alkaline waste than by an acid. The waste-siltstone combinations represented worst-case situations in which the wastes had not been diluted by formation waters. As with the sandstone, the behavior of dissolved silica for the siltstone could not be related to the solubility of a specific mineral. The thermodynamic models indicated that the solutions were undersaturated with respect to all silicate solid phases. The solution behavior of  $\text{Ca}^{2+}$  in the absence of brine appeared to be influenced by the solubility of calcite, but no clear carbonate equilibria were established.

Some chemical reactions could be described by thermodynamic modeling. In such cases, the observed concentration of inorganic constituents in solution appeared to be controlled by the solubility of common mineral phases. If the effects of temperature and pressure on mineral solubility are known, the extent of chemical interactions can be predicted if enough information is available on the mineralogical composition of the injection zone and the chemical composition of the waste and formation waters. In some waste-rock combinations, the solutions did not equilibrate with known mineral phases. Consequently, these investigations remained as empirical observations on waste-rock interactions, and elevated temperatures and pressures were required to more accurately simulate subsurface environments. The nonequilibrium conditions implied that some interaction studies require considerably longer periods of time than were possible in this project. Also, the specific computer-assisted models used to assess solution equilibria may be inappropriate for very concentrated solutions.

This study indicated that thermodynamic principles can predict simple geochemical interactions and that empirical laboratory-based investigations may be needed to complement an assessment of the fate of injected wastes. Some recommendations were formulated. When fate or compatibility demonstrations are necessary in the permitting process, subsurface temperatures and pressures should be included in the experimental design. Ideally, both a priori modeling and laboratory assessments should be used. Also, the contact time of the wastes with the core samples should be carefully considered: months or years may be required to attain chemical equilibrium. There are no well-documented procedures for conducting compatibility demonstrations. First-generation procedures were developed during this project that require further testing with other waste types.





## INTRODUCTION

Underground injection is the controlled emplacement of liquid wastes into geologic formations through specially designed and monitored wells. In Illinois, subsurface geologic formations have been used for waste disposal for about 20 years. Nine Class I injection wells, which include two standby wells, are currently in operation at seven industrial sites. A Class I well is used to inject municipal and industrial (hazardous and nonhazardous) wastes below underground sources of drinking water.

The Hazardous and Solid Waste Amendment of 1984 required that the U.S. EPA evaluate the environmental suitability of deep-well injection as a method of waste disposal. In Illinois in 1984, the State Legislature mandated a similar assessment of the regulations and practices of the Illinois Underground Injection Control (UIC) program as it relates to Class I hazardous waste disposal. The product of that assessment was a report by Brower et al. (1988), who concluded that the geochemical interactions between liquid wastes, formation waters, and the formations have not been well researched. Previous analyses also indicated that research was needed on geochemical interactions in order to predict and test the compatibility of the injected wastes with the formation and to assess the fate of injected wastes (Warner, 1965; van Everdingen and Freeze, 1971; Gordon and Bloom, 1984; LaMoreaux and Smith, 1985; Sullivan et al., 1986).

In a chemically incompatible waste-formation system, chemical precipitates or gases evolve during injection. Chemical precipitates can accumulate in the void spaces that make up the formation, reducing the formation's porosity. The reduced porosity leads to a reduction in injection efficiency, pressure buildup, and possibly the complete failure of the well. The accumulation of gaseous components, formed as reaction products, can also plug formation voids and reduce the permeability of the receiving formation as well as create excessive pressures in the formation that can lead to well "blowouts." Moreover, an analysis of deep-well injection systems by the Natural Resources Defense Council (Gordon and Bloom, 1984) concluded that a frequently occurring problem stems from the injection of liquid wastes that are chemically incompatible with the injection formations (including in situ brines). They felt that this incompatibility has caused the deterioration of the confining strata, allowing the migration of wastes from the injection zone.

Few studies on chemical compatibility have been conducted. In some of these studies, a liquid waste sample was mixed with a synthetic-formation water sample for 4 to 6 hours at room temperature and pressure. A mixture was considered compatible if it remained free of precipitates (Warner, 1965). Ostroff (1965) noted that some chemical reactions require considerably longer to go to completion and that other reaction products, such as gases, can cause a decrease in formation permeability. In some studies, the effects of formation temperatures and pressures on chemical interactions were ignored (Headlee, 1950; Bayazeed and Donaldson, 1971; and Barnes, 1972). In other studies, liquids injected to a depth of 900 meters were found to be subjected to hydrostatic pressures exceeding 10 MPa pressure and temperatures ranging from 50 to 100°C (Roedder, 1959; Bayazeed and Donaldson, 1973).

A few investigators have conducted laboratory experiments at elevated pressures and temperatures to simulate subsurface conditions. Goolsby (1972) conducted laboratory experiments with a waste sample containing organic monobasic and dibasic acids, nitric acid, sodium and ammonium salts, adiponitrile, hexamethylenediamine, alcohols, ketones, and esters. The waste liquid was mixed with disaggregated core samples of the Lower Limestone of the Florida Aquifer in a pressure vessel at 5.07 MPa. Details of the procedures used were not given, and formation temperatures were not considered. In one experiment, the pressure-vessel solution contained 3,000 mg Ca/L as the result of the dissolution of the limestone. After untreated (not neutralized) acid had been injected into an injection well, liquid samples collected from a monitoring well in the study area were found to contain 2,700 mg Ca/L. Consequently, the laboratory experiment appeared to have reasonably simulated field conditions. Goolsby (1972) also found that the amount of limestone that dissolved increased with reaction pressure with a concomitant decrease in solution pH.

Hower et al. (1972) conducted compatibility-type studies at 6.89 MPa and 43°C, but gave no procedural details. They found that adding HCl to a ferric chloride waste solution mixed with dolomite resulted in  $\text{Fe}(\text{OH})_3$  precipitation. Further experimentation showed that the addition of acetic or citric acid instead of HCl resulted in no iron precipitation. Gas evolution from the neutralization of the acid was not assessed.

Other studies have used flow-through systems rather than batch procedures to assess the chemical fate of injected wastes. Bayazeed and Donaldson (1973) examined the interaction of simulated acid wastes from steel processing composed of 12 percent  $\text{H}_2\text{SO}_4$  + 10 percent  $\text{FeSO}_4$  and 1 percent HCl + 8 percent  $\text{FeCl}_2$ . The simulated waste was hydraulically forced through core samples of the Mt. Simon Sandstone at ambient temperatures. The acidity of the waste solutions was not significantly reduced, but solution iron was reduced. Bayazeed and Donaldson (1973) concluded that after a long period of storage most of the acid would be neutralized. However, they did not provide any supporting evidence.

Donaldson and Johansen (1973) subjected core samples of the Cottage Grove Sandstone from Oklahoma to 60°C and 20.3 MPa using an autoclave. The core samples were initially saturated with aqueous solutions containing various organic compounds. Butanol, *n*-hexylamine, and phenol were adsorbed by the sandstone. On the basis of these experiments, Donaldson and Johansen (1973) concluded that the migration of these organic compounds in the subsurface would be retarded by adsorptive interactions with the injection formation.

To circumvent addressing the chemical interactions of specific waste-formation systems by laboratory studies, some investigators have attempted to use computer-assisted transport and chemical (thermodynamically based) models to assess the fate and distribution of chemical constituents in injection scenarios. Scrivner et al. (1986) summarized that the chemical fate of injected wastes can be determined by "standard chemical engineering techniques," and that the concentrations of hazardous constituents are typically reduced by reactions within the waste or the injection environment. Scrivner and his co-workers at E. I. du Pont de Nemours and Company have used computer simulations to model the fate of injected hazardous wastes. The models considered reaction rates and the equilibrium constants for the dominant reactions. Validation of the du Pont model has not been demonstrated, and the model was not publically available.

In an analysis of the concept of modeling geochemical interactions in deep-well systems, Sullivan et al. (1986) warned that accurate thermodynamic data are lacking for many heterogeneous solid wastes and chemical interactions. They noted that kinetic data for many reactions under elevated temperature and pressure are unknown. Sullivan et al. determined that thermodynamic models could be applied only tenuously to predict the fate of injected wastes. Brower et al. (1988) concluded that laboratory compatibility studies on chemical interactions have a better predictive value than equilibrium models.

In summary, few laboratory experiments have been conducted on the chemical compatibility and fate of injected hazardous wastes. Comprehensive geochemical models for hazardous waste injection are emerging, but none have been validated. The U.S. Environmental Protection Agency critically evaluated the environmental suitability of Class I well injection of hazardous wastes and proposed that untreated wastes be banned from injection (U.S. EPA, 1987, 1988). However, the U.S. EPA has proposed two circumstances whereby operators may petition the Administrator to obtain a permit to inject waste liquids:

1. Using hydrogeologic flow and transport models, the applicant could demonstrate that injected fluids would not migrate vertically upward out of the injection zone or migrate within the injection zone to a point of discharge over a time span of 10,000 years. The EPA has interpreted "no migration" as containment for 10,000 years.



2. The applicant could demonstrate that a hazardous waste would be transformed into a nonhazardous waste within the injection zone by neutralization (e.g., mixing acids with carbonates), adsorption (e.g., immobilization of hazardous constituents by clay minerals), degradation, and/or other mechanisms.

The second demonstration is the policy context of this study. The U.S. EPA expressed the belief that fluid-flow demonstrations could be more easily conducted than waste-transformation demonstrations because the state-of-knowledge of the latter is not as advanced. This project was initiated to contribute to waste-transformation studies.

## EXPERIMENTAL OBJECTIVES AND APPROACH

The overall objective of this project was to develop basic geochemical data that would lead to a more complete understanding of inorganic physicochemical interactions of liquid hazardous wastes with subsurface-injection strata and associated brines. The approach to accomplish this objective was to undertake compatibility-type studies using batch-pressure reaction vessels operated in temperature-controlled water baths to represent subsurface temperature-pressure regimes. Disaggregated core samples of the Mt. Simon Sandstone, Potosi Dolomite, and Eau Claire Formation were mixed with selected liquid-waste samples currently injected in Illinois.

The waste-formation interaction studies were conducted in Parr 600-mL stirred pressure vessels made of either stainless steel T316 (65 percent Fe, 17 percent Cr, 12 percent Ni, 2.5 percent Mo, 2 percent Mn, and 1 percent Si) or Hastelloy B-2 (66 percent Ni; 28 percent Mo; 2 percent Fe; and 1 percent Cr, Mn, and Co). Details of the procedures are given in Appendix B. A 1:4 solid-to-liquid ratio (wt/vol) was used in the studies. Fifty grams of disaggregated core sample (<2 mm size fraction) and 200 mL of the liquid waste were placed into each vessel. The assembled vessels were evacuated and purged with nitrogen before liquid was added, so that an oxygen-poor atmosphere would be created, minimizing oxidation reactions. The nitrogen concentration in the head space prior to the addition of the liquid typically ranged from 97 percent to 99 percent N<sub>2</sub>, while the oxygen content ranged from 1 to 3 percent O<sub>2</sub>.

The liquid samples were added to the pressure vessels with a glass syringe, allowing the vessels to remain free of exposure to the atmosphere. The vessels were pressurized using N<sub>2</sub>, set into a water bath, and periodically stirred. When the specific experiment was completed, liquid samples were collected from the vessels by allowing the internal pressure to push the liquid through an in-line filter. The vessels were then depressurized, and post-contact gas samples were collected. The pressure vessels were simultaneously heated and pressurized to simulate subsurface conditions corresponding to different depths,

Temperature	Pressure	Approximate depth
298°K (77°F)	0.1 MPa (0 psig)	Surface
313°K (104°F)	6.0 MPa (871 psig)	457 m (1500 ft)
328°K (131°F)	11.7 MPa (1697 psig)	914 m (3000 ft)

Injection zones in Illinois range in depth from approximately 470 to 1680 meters. The conditions selected in this study represented the widest range in temperature and pressure for which the pressure vessels could be safely operated. The vessels could not be pressurized to exceed 11.7 MPa (1697 psig) without risking failure of the rupture discs (safety devices). Surface conditions were included for comparisons with data generated by the simulated-subsurface conditions. Temperature and pressure were not varied independently.

The experiments were conducted with six waste-formation combinations for 15 days. The vessels were used as batch reactors, and were terminated after 3, 6, 9, 12, and 15 days. Exemplary replicates were conducted with selected systems at 328°K-11.7 MPa.

Although the major emphasis of this project was to observe and interpret interactions between the waste solutions and the formations, additional experiments were conducted at 328°-11.7 MPa with a formation brine-waste mixture. This brine-waste mixture (1:1, vol/vol) was mixed for 15 days with each disaggregated core sample to represent the mixing front in deep-well environments. The brine was included in this study to investigate effects of a formation water on reaction equilibria.

## ANALYTICAL METHODS

The solution concentrations of  $\text{Cl}^-$ ,  $\text{F}^-$ ,  $\text{NO}_3^-$ ,  $\text{SO}_4^{2-}$ , and  $\text{Fe}^{3+}$  were determined using a Dionex 2110i ion chromatograph. Anions were separated using a 2.3 mM sodium carbonate-2.9 mM sodium bicarbonate eluant at a flow rate of 2 mL/min through Dionex AS-4 and AS-5 columns. Quantification was accomplished by measuring the electrical conductivity of the eluant-anion mixture. Quality control standards obtained from the U.S. EPA (table 1) were used to verify results at the time of analysis.

**Table 1** Quality assurance-quality control standards used in this project

---

U.S. Environmental Protection Agency  
Environmental Monitoring and Support Laboratory

Trace Metals I	ICAP-23
Trace Metals II	ICAP-INTER 3
Trace Metals III	ICAP-INTER 5
Water Pollution Control	ICAP-INTER 18
ICAP-7	MINERAL
ICAP-19	Nitrate/fluoride

Environmental Resource Associates (ERA)

Minerals WasteWatR™  
Hardness WasteWatR  
Trace Metals WasteWatR

---

A Dionex CS-5 analytical column and an eluant composed of 6 mM pyridine-dicarboxylic acid (PDCA), 50 mM acetic acid, and 50 mM sodium acetate was used to separate  $\text{Fe}^{3+}$  from the other ionic constituents at a flow rate of 1 mL/min. The eluant-iron mixture was then passed through a post-column membrane reactor in which a PAR solution (0.2 mM 4(2-pyridylazo)-resorcinol-3 M  $\text{NH}_4\text{OH}$ -1 M acetic acid) was continuously added, and reacted with the iron-PDCA complex. The reacted complex was quantified with a UV-Vis spectrophotometric detector. A stock  $\text{Fe}^{3+}$  solution was prepared with iron (III) nitrate nonahydrate ( $\text{Fe}(\text{NO}_3)_3 \cdot 9\text{H}_2\text{O}$ ) in a degassed 1 percent perchloric acid solution. The standard solutions were made using a diluent that had an anion matrix similar to that of the samples.

The solution concentrations of total Al, As, B, Ba, Ca, Cd, Co, Cr, Cu, Fe, K, Mg, Mn, Mo, Na, Ni, P, Pb, Sb, Se, Si, Sn, V, and Zn were determined using an inductively coupled argon plasma (ICAP) emission spectrophotometer (Jarrell-Ash 975 AtomComp). The instrument was standardized using certified solutions prepared by Inorganic Ventures, Inc. Quality control standards obtained from the U.S. EPA (table 1) were used to verify results during each analysis. This instrument has a DEC PDP-8A central processing unit that performs interelement correction and automatic background correction of individual spectral intensities.

A summary of QA/QC statistics is given in table 2. The detection limits for the ICAP constituents were determined as three times the standard deviation of each mean for each constituent measured in deionized water. The detection limits for the ion chromatograph (i.e., Cl, F,  $\text{NO}_3$ ,



and SO<sub>4</sub>) were estimated empirically. The mean percent bias was calculated as the mean of the absolute value of the measured concentration minus the true concentration divided by the true concentration. The summary statistics are applicable to the analytical ranges given (table 2). Hence, the laboratory samples were diluted when needed such that the concentration of the analyte was in the optimum range. Each sample was analyzed at least twice. Multiple analyses were conducted in most cases, particularly those that were known to have a high (>4 percent) coefficient of variation, such as sodium and silica. In general, the percent bias and variation were less than 10 percent for those constituents studied in this project.

Samples of the alkaline liquid were analyzed by gas chromatography-mass spectroscopy by the Institute for Environmental Studies of the University of Illinois. One liter of the waste was

**Table 2** Detection limits, percent bias, and coefficient of variation for each constituent and the variance associated with the samples

Constituent	Common detection limit	% Bias (mean ± SD)		Common % CV for QA stds.	No. of data	Applicable range (mg/L)	Range in CV assoc. with samples
Aluminum (Al)	0.05	10.5	9.32	6	18	0.1-60.0	3.5-7.6
Arsenic (As)	0.05	6.91	4.60	5	35	0.1-1.0	0-20.2
Boron (B)	0.08	1.14	1.25	2	4	0.1-10.0	0.7-7.6
Barium (Ba)	0.06	4.28	2.76	0.5	15	0.1-50.0	0-1.7
Beryllium (Be)	0.01	5.70	2.22	3	30	0.1-2.00	NA <sup>a</sup>
Calcium (Ca)	0.01	2.06	2.67	4	12	0.1-50.0	1.8-9.90
		4.37	1.58	4	16	50.0-300	
Cadmium (Cd)	0.03	4.65	3.34	5	19	0.1-1.00	0.3-7.21
Chlorine (Cl)	0.20	2.89	2.9	1	31	30-70	0.01-8.1
Cobalt (Co)	0.04	2.94	2.56	2	32	0.1-3.0	NA
Chromium (Cr)	0.03	15.7	11.2	5	24	0.1-3.0	0.20-9.12
Copper (Cu)	0.05	5.71	4.79	2	31	0.1-3.0	2.10-8.13
Fluorine (F)	0.20	8.94	5.09	3	23	1-4.00	0.03-8.00
Iron (Fe)	0.05	3.99	2.90	3	32	0.1-10.0	0-5.37
Potassium (K)	0.08	7.53	6.05	12	12	1-50	5.2-15.7
		5.14	0.19	5	9	50-200	
Magnesium (Mg)	0.07	3.34	2.81	6	24	1-15	1.72-10.7
Manganese (Mn)	0.01	4.1	2.56	3	24	0.1-3.5	3.72-9.28
Molybdenum (Mo)	0.02	9.62	14.5	6	21	0.1-50	5.42-12.7
Sodium (Na)	1.00	25.0	15.5	- <sup>b</sup>	10	1-10	4.52-13.7
		- <sup>c</sup>	-	1-10	26	10-300	
Nickel (Ni)	0.03	4.73	2.66	4	34	0.1-2.00	1.7-9.82
Nitrate (NO <sub>3</sub> )	0.30	2.84	2.04	3.5	35	1-50	0.04-9.50
Oxygen (O <sub>2</sub> )	- <sup>d</sup>	- <sup>e</sup>	-	-	-	-	7.40-13.5
Phosphorus (P)	0.05	- <sup>d</sup>	-	-	-	-	NA
Lead (Pb)	0.03	4.18	4.18	3	14	0.40-4.0	2.30-6.17
Silicon (Si)	0.20	12.7	8.71	5	7	5-20	4.92-13.2
Sulfate (SO <sub>4</sub> )	0.30	5.20	3.54	1.5	29	1-10	0.1-8.9
Zinc (Zn)	0.05	6.32	1.96	3	12	1-4	0.7-13.7

<sup>a</sup>Not applicable; constituent not detected in solution.

<sup>b</sup>Extremely variable (1 to 40%) at low (<10 mg/L) concentrations.

<sup>c</sup>Extremely variable (0 to 24%); requires analytical considerable skill.

<sup>d</sup>Not assessed.

<sup>e</sup>No QA/QC standard available.

extracted three times with 60 mL of methylene chloride to generate the neutral-base fraction. The three 60-mL extracts were combined. A sample of this combined solution was then adjusted to a pH of less than 2, then extracted with methylene chloride, generating an acid fraction. Both extracts were then concentrated using a Snyder column. The gas chromatograph (GC) conditions included temperature programming over the range 60-280°C at 3°C/min, with an initial hold time of 12 minutes at 60°C. The GC column was a model DB-1 (J. and W. Scientific) 30 m x 0.32 mm ID. The mass spectrometer was operated in an electron ionization mode at 70 eV. Peaks were identified by matching them with library spectra and by deductive interpretation.

Volatile organic compounds were determined by direct GC injection via a Tekmar liquid sample concentrator. The GC column was 2.44 m x 2 mm ID glass, and contained 1 percent SP-1000 60/80 Carboxpack. The initial injection temperature was 45°C, temperature programmed at 8°C/min to 220°C, with a hold time of 20 minutes.

The heats-of-reaction between the liquid wastes and the disaggregated samples were determined with a Parr 1451 solution calorimeter. The instrument was standardized with tris(hydroxymethyl)-aminomethane dissolved in a 0.1N HCl solution. The core samples were fine ground (<20 µm) prior to analysis, and 0.7 to 1.6 g was equilibrated with 100 mL of the liquid waste. The equilibration time varied from 3 to 14 minutes depending on the sample-liquid mixture. Further details on procedures and the theory of operation are given in Ramette (1984).

The mineralogical composition of the three core samples was determined by X-ray diffraction with a Phillips Norelco X-ray diffractometer using Cu-K $\alpha$  radiation and a graphite monochromometer at 40 kV and 20 mA. This approach is discussed further in Russell and Rimmer (1979). Scans were conducted on randomly oriented bulk samples at a rate of 2 degrees-2 $\theta$ /min. The clay fraction (<2 µm) was prepared by dispersing the sample in water. About 2 mL was extracted from the upper 1 cm of the suspension, and placed on a glass petrographic slide and allowed to air dry. The clay slides were X-rayed after solvation with ethylene glycol and heating to 375°C. Quantification was conducted by using illite as an internal standard.

Particle-size determinations were conducted with a Micromeritics 5000ET SediGraph. This instrument measures the sedimentation rate of particles in solution and interprets these data in accordance with Stoke's Law to yield equivalent-spherical diameters.

The gas samples were characterized with a Perkin-Elmer Sigma I gas chromatograph that was equipped with flame ionization and thermal conductivity detectors and an Alltech CTR1 column. This column was capable of separating CO, CO<sub>2</sub>, N<sub>2</sub>, NH<sub>4</sub>, and O<sub>2</sub> from gas mixtures. The relative concentration of each gas component was determined by dividing the individual peak areas by the total peak area. Identification of peaks was verified by gas standards purchased from Alltech Associates, Incorporated.

The oxidation-reduction potential (Eh), pH, and electrical conductivity of the solutions were measured by electrode (American Public Health Association, 1975) and where possible, checked with ERA standards (table 1). Instrument calibration was performed with solutions at the same temperatures as the samples. The potassium ferric-ferrocyanide solution described by ZoBell (1946) was used as an Eh reference solution (see Wood, 1976). Dissolved oxygen was determined using a YSI (Yellow Springs Instrument Co.) Model 58 meter. The instrument was calibrated using the air-saturated water technique corrected for temperature, altitude, and salinity.

### **Characterization of the Core Samples**

Sandstone and carbonates are the two major types of injection materials in Illinois, and in the U.S. (Warner and Lehr, 1977). Therefore, the Potosi Dolomite and the Mt. Simon Sandstone were selected for this study. Both formations are Cambrian-age marine deposits that underlie most of Illinois and are used for deep-well injection of liquid wastes (see Brower et al., 1988).



Samples of the Potosi Dolomite were selected from a core drilled for natural gas storage in Kankakee County, Illinois (Sec. 28, Twp. 30 N., Range 10 East). A geological description of each of the sampled intervals is given in Appendix C. The Proviso member of the Eau Claire Formation was also sampled from the same core. Samples of the Mt. Simon Sandstone were collected from the Mahesius No. 1 core drilled in La Salle County (32-35N-1E) by the Northern Illinois Gas Company. The stratigraphic relationship of the three formations sampled is shown in figure 1. For each rock type, 20 kg of rock was collected from the entire core interval, combined and disaggregated with a Roll rock crusher, and ground to pass through a 2-mm sieve. This material was then mixed and subdivided using a sample splitter to produce a series of representative subsamples of each bulk sample. Consequently, one mixed sample of each core interval was generated to represent the sampled interval. The samples were coarse-grained (table 3) and were used in this form.

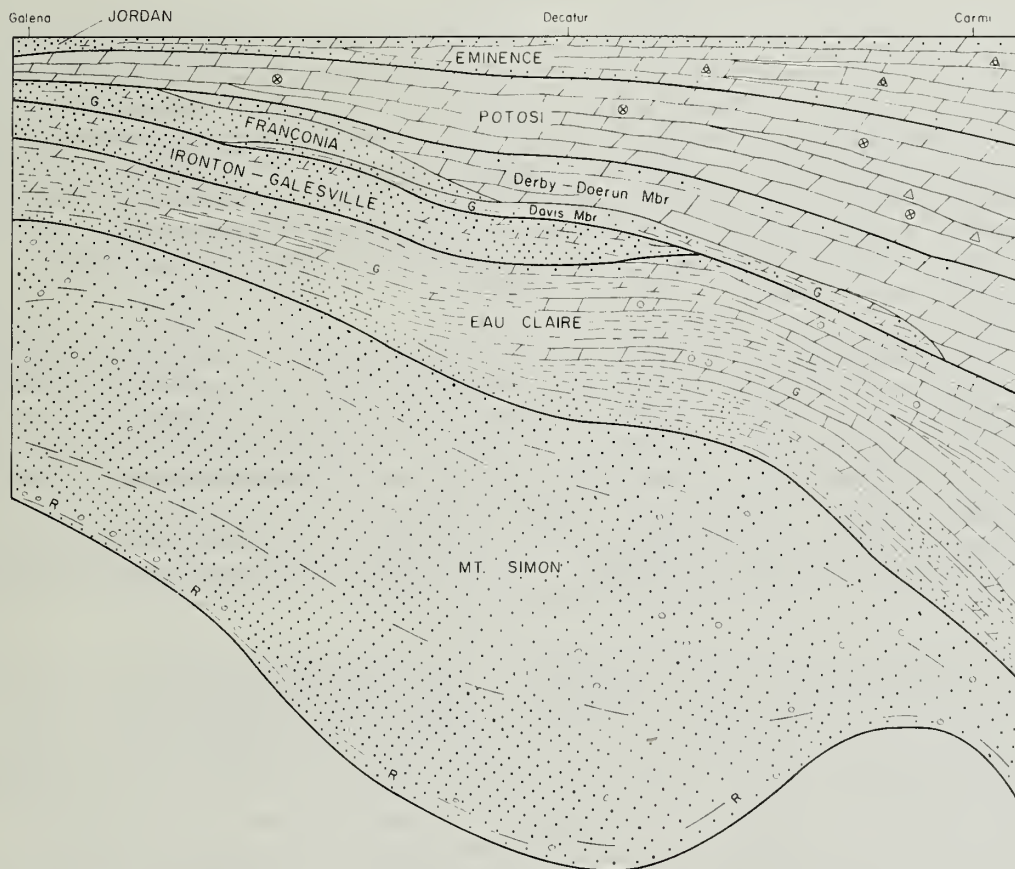


**Figure 1** Stratigraphic relationships between the Potosi Dolomite, Eau Claire Formation, and Mt. Simon Sandstone from northwestern to southeastern Illinois (Willman et al., 1975).

**Table 3** Particle-size data for the three disaggregated core samples (percent weight)

Size fraction ( $\mu\text{m}$ )	Mt. Simon Sandstone	Potosi Dolomite	Proviso Siltstone
>53-2000	95.7	87.0	68.8
31-53	0.8	4.3	9.4
16-<31	0.5	3.1	7.2
8-<16	0.4	2.2	3.7
4-<8	0.5	1.6	2.8
2-<4	0.5	1.0	2.5
<2	1.6	0.8	5.6

The Potosi Dolomite is a finely crystalline, pure to slightly argillaceous dolomite that ranges in thickness from 30 to 90 meters (Willman et al., 1975). On the basis of semiquantative X-ray diffractometry (XRD) data, the Potosi Dolomite sample was determined to be an essentially pure dolomite (95 percent) with approximately 5 percent quartz. The Mt. Simon Sandstone ranges from less than 152 meters to approximately 790 meters in thickness. The formation consists of fine-to-coarse grained, partly pebbly, friable sandstone. The bulk sample was approximately 90 percent quartz, 6 percent potassium feldspar, less than 5 percent phyllosilicates (clays), and a trace of dolomite. The phyllosilicates were about 75 percent illite, 20 percent mixed-layer illite/smectite, 5 percent smectite, and a trace of chlorite.

The Mt. Simon Sandstone is overlain by the Eau Claire Formation (fig. 1). The Proviso Siltstone Member of the Eau Claire Formation was used to examine reactions with a unit that would serve as a confining layer (cap rock) in a deep-well scenario. The Eau Claire Formation is used as the upper confining layer at two deep-well injection facilities in Illinois (Brower et al., 1988). The siltstone is approximately 46 to 90 meters thick and is dominantly a dolomitic, sandy, feldspathic, slightly glauconitic siltstone (Willman et al., 1975). The Proviso sample was composed of approximately 50 percent quartz, 25 percent potassium feldspar, 15 percent dolomite, and 10 percent phyllosilicates as determined by XRD. The phyllosilicates were approximately 87 percent illite, 7 percent chlorite, and 6 percent mixed-layer illite/smectite.

#### **Chemical Characterization of the Acidic Waste**

An acidic, inorganic liquid waste was collected from the Cabot Corporation plant near Tuscola, Illinois. Approximately 20 liters was collected from a storage tank using Pyrex carboys. The carboys were capped and stored at 4°C. The waste liquid was a by-product from the production of a high-purity amorphous silica. The solution contained 0.09 percent HCl by NaOH equivalency (Bergonson, 1988). The acidic solution is injected at the plant into a zone including the basal portion of the Eminence Formation (dominantly dolomitic), and the upper part of the Potosi Dolomite. Chemical characterization of the 40-liter sample (table 4) indicated that it was a dilute, oxidized solution with an ionic strength of 0.009 moles/L. During the course of the project, the solution was fairly stable chemically. The solution became less oxidized during the 6-month interval, and the pH decreased slightly. Although the solution concentrations of some constituents changed, the changes were minor and did not complicate the interpretation of the interaction studies.

#### **Chemical Characterization of the Alkaline Waste**

Approximately 40 liters of an alkaline liquid waste was collected from the Velsicol Chemical Corporation at Marshall, Illinois. The samples were also collected from a storage tank using Pyrex carboys and were wrapped with aluminum foil to prevent photodegradation. These samples were stored under ambient conditions, since brine-like solutions (such as this waste) are less



**Table 4** Chemical composition of the acidic waste sample (the same solution was analyzed at three dates during the project)

	January 1987	April 1987	June 1987
pH	2.03	1.90	1.94
Eh <sub>z</sub> <sup>a</sup>	+1338	+800	+817
EC (mmhos/cm) <sup>b</sup>	7.22	6.89	5.89
Aluminum (Al) <sup>c</sup>	8.61	9.09	8.90
Arsenic (As)	<0.05	0.06	0.07
Boron (B)	<0.08	0.08	0.12
Barium (Ba)	<0.01	0.05	0.06
Beryllium (Be)	<0.01	<0.01	<0.01
Calcium (Ca)	83.9	89.9	92.9
Cadmium (Cd)	<0.03	<0.03	<0.03
Chlorine (Cl)	829	892	878
Cobalt (Co)	0.14	0.15	0.18
Chromium (Cr)	<0.02	<0.02	<0.02
Copper (Cu)	<0.05	<0.05	<0.05
Fluorine (F)	0.48	0.67	0.75
Iron (Fe)	23.5	25.5	24.9
Potassium (K)	2.62	3.03	3.04
Magnesium (Mg)	34.6	37.3	38.0
Manganese (Mn)	1.34	1.23	1.51
Molybdenum (Mo)	<0.02	<0.02	<0.02
Sodium (Na)	15.6	15.2	14.1
Nickel (Ni)	<0.03	<0.03	<0.03
Nitrate (NO <sub>3</sub> )	46.7	42.0	43.2
Oxygen (dissolved O <sub>2</sub> )	6.0	6.3	6.4
Phosphorus (P)	0.11	0.05	0.10
Lead (Pb)	<0.03	<0.03	<0.03
Silicon (Si)	6.41	5.92	7.23
Sulfate (SO <sub>4</sub> )	121	150	119
Zinc (Zn)	<0.04	0.22	0.45

<sup>a</sup>Referenced to a ZoBell solution.  
<sup>b</sup>Electrical conductivity; temperature corrected.  
<sup>c</sup>Total mg/L.

soluble at lower temperatures. The sample collected was the caustic process water from pesticide manufacturing. This alkaline waste is currently injected into a Devonian limestone at the Marshall plant. The upper confining unit is the New Albany Shale, and the Maquoketa Shale serves as the lower confining unit.

As previously mentioned, the waste was essentially a brine-like solution (table 5) with an ionic strength of approximately 4.6 moles/L. This solution was frequently diluted prior to injection with contaminated surface runoff and accumulated storm waters at a ratio of approximately 1:5, waste to runoff. All experiments in this study were conducted with the undiluted waste. The 40-liter sample was relatively stable during the course of the project. During an 8-month interval, for example, the pH of the undiluted waste fluctuated between 12.6 and 13.3 with no discernible trend and may have been due to analytical error (table 5). The solution concentrations of total

**Table 5** Inorganic chemical composition of the alkaline waste sample (the same solution was analyzed at four dates during the project)

	October 1986	January 1987	April 1987	June 1987
pH	12.9	12.6	13.3	12.6
Ehz (mV) <sup>a</sup>	+572	+611	+594	+606
EC (mmhos/cm) <sup>b</sup>	403	413	410	335
Pheno. alkalinity <sup>c</sup>	17,880	18,160	19,940	17,920
Total alkalinity <sup>c</sup>	22,030	21,190	23,490	21,550
Aluminum <sup>d</sup>	0.65	0.61	0.71	2.90
Arsenic	<0.05	<0.05	<0.05	<0.05
Boron	<0.08	<0.08	0.55	7.36
Barium	<0.06	<0.06	<0.08	<0.06
Beryllium	<0.01	<0.01	<0.01	<0.01
Calcium	1.06	1.14	1.21	1.00
Cadmium	<0.03	<0.03	<0.03	<0.03
Chlorine	112,660	108,000	105,000	105,000
Cobalt	<0.04	<0.04	<0.04	<0.04
Chromium	0.03	0.03	0.03	<0.03
Copper	<0.05	<0.05	<0.05	<0.05
Fluorine	151	166	161	156
Iron	0.43	0.59	0.58	0.47
Potassium	50.9	51.5	71.0	34.1
Magnesium	<0.07	<0.07	<0.07	<0.07
Manganese	<0.01	<0.01	<0.01	<0.01
Molybdenum	0.33	0.27	0.10	0.06
Sodium	86,350	83,860	85,700	84,000
Nickel	<0.03	<0.03	<0.03	<0.03
Nitrate	274	257	246	242
Oxygen	4.9	4.2	3.9	2.4
Phosphorus	0.65	0.44	0.21	0.12
Lead	<0.03	<0.03	<0.03	<0.03
Silicon	10.7	13.9	8.61	10.8
Sulfate	62.0	65.0	71.0	89.9
Zinc	<0.05	<0.05	<0.05	<0.05

<sup>a</sup>Referenced to a ZoBell solution.

<sup>b</sup>Electrical conductivity; temperature corrected.

<sup>c</sup>Reported as mg/L calcium carbonate.

<sup>d</sup>Total mg/L.

Al, B, and SO<sub>4</sub> increased during this interval, whereas the concentrations of total Cl, Mo, NO<sub>3</sub>, dissolved O<sub>2</sub>, and P decreased. Comparisons with QA/QC data (table 2) indicated that the changes in concentration were not due to analytical error. None of the changes in solution composition complicated the interpretation of the interaction studies.

The major emphasis of this study was inorganic chemical interactions. In addition, to contribute to the database on the organic composition of injected-hazardous wastes, the waste was qualitatively characterized in terms of its organic composition. The open literature presents few such data.

**Table 6** Gas chromatographic-mass spectrometric analysis of the base-neutral fraction of the alkaline waste

Peak no.	Retention time (min)	Compound	Formula	Molecular weight
1	5.6	Chlorocyclohexanol	C <sub>6</sub> H <sub>6</sub> ClO	134
2	7.4	Dichlorocyclohexane	C <sub>6</sub> H <sub>10</sub> Cl <sub>2</sub>	152
3	8.4	Trichlorocyclopentane or trichloropentene	C <sub>5</sub> H <sub>7</sub> Cl <sub>3</sub>	172
4	8.7	Dichlorocyclopentene?	C <sub>5</sub> H <sub>6</sub> Cl <sub>2</sub>	136
5	9.3	Tetrachlorocyclopentadiene	C <sub>5</sub> H <sub>2</sub> Cl <sub>4</sub>	202
6	9.5	Tetrachlorocyclopentadiene	C <sub>5</sub> H <sub>2</sub> Cl <sub>4</sub>	202
7	13.0	Tetrachlorocyclopentadiene	C <sub>5</sub> H <sub>2</sub> Cl <sub>4</sub>	202
8	15.0	Tetrachloropentene or tetrachlorocyclopentane	C <sub>5</sub> H <sub>6</sub> Cl <sub>4</sub>	206
9	15.5	Unknown	Unknown	Unknown
10	17.1	Tetrachlorocyclopentene?	C <sub>5</sub> H <sub>5</sub> Cl <sub>4</sub>	204
11	17.8	Unknown (chlorinated)	Unknown	Unknown
12	18.4	Pentachlorocyclopentadiene	C <sub>5</sub> HCl <sub>5</sub>	236
13	18.7	Pentachlorocyclopentadiene	C <sub>5</sub> HCl <sub>5</sub>	236
14	25.1	Hexachlorocyclopentadiene	C <sub>5</sub> Cl <sub>6</sub>	270
15	29.4	Unknown (with 4 or 5 chlorines)	Unknown	Unknown
16	29.6	Unknown	Unknown	Unknown
17	30.2	Trichlorocyclohexadiene	C <sub>6</sub> H <sub>5</sub> Cl <sub>3</sub>	182
18	33.7	Unknown (with 1 chlorine)	Unknown	226?
19	34.4	Unknown	Unknown	Unknown
20	36.1	Unknown	Unknown	Unknown
21	39.1	Unknown (with chlorine and carbonyl)	Unknown	216?
22	39.7	Unknown	Unknown	Unknown
23	40.1	Unknown	Unknown	Unknown
24	43.3	Tetrahydromethanoindene	C <sub>10</sub> H <sub>6</sub> Cl <sub>6</sub>	336
25	43.5	Unknown (chlorinated)	Unknown	Unknown
26	44.6	Unknown (with at least 3 chlorines)	Unknown	266?
27	45.0	Unknown	Unknown	Unknown
28	46.5	Unknown (with at least 4 chlorines)	Unknown	301?
29	46.8	Unknown (with 4 chlorines)	Unknown	264?
30	47.1	Unknown	C <sub>6</sub> Cl <sub>6</sub>	282
31	48.2	Unknown (with 4 chlorines)	Unknown	Unknown
32	48.5	Unknown	C <sub>6</sub> Cl <sub>6</sub>	282
33	49.4	Phthalate	Unknown	Unknown
34	51.2	Unknown (with 4 or 5 chlorines)	Unknown	316?
35	66.4	Phthalate	Unknown	Unknown
36	66.7	Diisopropenyldimethylcyclohexane	C <sub>12</sub> H <sub>24</sub>	192

The waste was extracted with methylene chloride to generate a base-neutral fraction (table 6). Fifteen of 36 peaks were identified. The major organic components were hexachlorocyclopentadiene (C-56), pentachlorocyclopentadiene, and tetrachlorocyclopentadiene.

Fewer compounds were detected in the acidic fraction (table 7), which consisted of mostly chlorinated compounds. Volatile organics (table 8) were also dominated by halogenated hydrocarbons. Organic characterizations of the solutions generated during the interaction studies were not conducted.



**Table 7** Gas chromatographic-mass spectrometric analysis of the acid fraction of the alkaline waste

Peak no.	Retention time (min)	Compound	Formula	Molecular weight
1	5.1	Chlorotrimethylcyclopropane	C <sub>6</sub> H <sub>11</sub> Cl	118
2	5.3	Dichlorocyclohexane	C <sub>6</sub> H <sub>10</sub> Cl <sub>2</sub>	152?
3	5.7	Chlorocyclohexanol	C <sub>6</sub> H <sub>11</sub> ClO	134
4	5.8	Unknown (with Cl and COOH)	Unknown	134
5	7.5	Dichlorocyclohexane	C <sub>6</sub> H <sub>10</sub> Cl <sub>2</sub>	152
6	8.0	Chlorocyclohexane	C <sub>6</sub> H <sub>11</sub> Cl	118
7	17.2	Unknown (with 4 chlorines)	C <sub>5</sub> H <sub>2</sub> Cl <sub>4</sub> ?	202
8	17.5	Dichlorocyclohexane	C <sub>6</sub> H <sub>10</sub> Cl <sub>2</sub>	152
9	19.2	Dichlorocyclohexene?	C <sub>6</sub> H <sub>9</sub> Cl <sub>2</sub>	150
10	19.8	Trichlorocyclohexene?	C <sub>6</sub> H <sub>7</sub> Cl <sub>3</sub>	184
11	21.3	Trichlorocyclohexane?	C <sub>6</sub> H <sub>10</sub> Cl <sub>3</sub>	186
12	27.7	Trichlorocyclohexene?	C <sub>6</sub> H <sub>7</sub> Cl <sub>3</sub>	184
13	29.2	Trichlorocyclohexene?	C <sub>6</sub> H <sub>7</sub> Cl <sub>3</sub>	184
14	31.0	Trichlorocyclohexene?	C <sub>6</sub> H <sub>7</sub> Cl <sub>3</sub>	184
15	38.6	Unknown (with 3 chlorines)	Unknown	Unknown

**Table 8** Gas chromatographic analysis of the alkaline waste: volatile organic compound detected

Chloroform (CHCl <sub>3</sub> )
1,1-Dichloroethane (C <sub>2</sub> H <sub>4</sub> Cl <sub>2</sub> )
Carbon tetrachloride (CCl <sub>4</sub> )
Trichloroethene (C <sub>2</sub> HCl <sub>3</sub> )
Bromoform (CHBr <sub>3</sub> )
Tetrachloroethene (C <sub>2</sub> Cl <sub>4</sub> )
Benzene (C <sub>6</sub> H <sub>6</sub> )
Toluene (C <sub>6</sub> H <sub>5</sub> CH <sub>3</sub> )
Ethylbenzene (C <sub>6</sub> H <sub>5</sub> C <sub>2</sub> H <sub>5</sub> )
o-Xylene (1,2-C <sub>6</sub> H <sub>4</sub> (CH <sub>3</sub> ) <sub>2</sub> )

### Chemical Characterization of the Connate Formation Brine

A connate formation brine sample was collected from the injection zone at the Velsicol site. Five liters of solution was collected with a steel bailer from an observation well at a depth of approximately 730 meters in Devonian limestones. The brine sample was stored under nitrogen in the field at 345 Pa in a stainless steel pressure canister to minimize oxidation and degassing.

The brine was alkaline and very reduced (table 9), and tended to oxidize quickly when removed from the pressure canister. The brine was composed mostly of sodium and chloride and had a total dissolved solids content of approximately 22,000 mg/L. The chemical composition of this brine sample was comparable to a sample collected by Meents et al. (1952) from the same county (Clark) from a depth of approximately 635 meters. Comparisons with Illinois State

Geological Survey (ISGS) data on the chemical composition of samples collected from the Velsicol observation well (table 9) suggested that the brine sample was representative in terms of pH and chloride concentrations of the formation fluids collected during the last 8 years. Compositional data collected by the Illinois State Water Survey (ISWS) suggested that brine samples collected at the Velsicol plant have contained higher concentrations of iron in the past.

Table 9 Chemical composition of formation brine samples collected from the Velsicol observation well

	This study	Meents et al., 1952 <sup>a</sup>	ISGS files, 1977-1985	ISWS files, 1972-1973
pH	9.07	7.7	7.1-10.7	
Eh <sub>2</sub> (mV)	-154	- <sup>b</sup>	(mean, 8.1)	
EC (mmhos/cm)	22.0	-		
Pheno. alkalinity <sup>c</sup>	66.0	0		
Total alkalinity <sup>c</sup>	380	573		476-860
Total dissolved solids (mg/L)	22,000	11,994	15,300-28,100 (mean, 19,680)	17,000-17,700
Aluminum <sup>d</sup>	0.09	ND <sup>e</sup>		
Arsenic	<0.05	-		
Boron	4.00	-	2.2-87.5	
Barium	0.81	-	(mean, 4.71)	0.3-0.9
Beryllium	<0.01	-		
Calcium	147	329		
Cadmium	<0.03	-		<0.01
Chlorine	12,700	6,603	8,740-22,300	8,200-9,440
Cobalt	<0.03	-	(mean, 12,500)	
Chromium	0.26	-		0.01-0.03
Copper	<0.03	-		0.02-0.03
Fluorine	20.1	-		
Iron	0.12	ND	6.9-91.0	
Potassium	72.8	-		
Magnesium	117.0	196		
Manganese	0.14	ND		
Molybdenum	0.07	-		
Sodium	8,370	3,763		
Nickel	<0.05	-		
Nitrate	25.1	44		
Phosphorus	0.08	-		
Lead	<0.03	-		<0.05-0.17
Silicon	7.87	2.34		
Sulfate	182	193		14.8-391
Zinc	<0.03	-		0.03-0.07

<sup>a</sup>Brine sample collected from the same area, but not from the Velsicol well.

<sup>b</sup>No value given.

<sup>c</sup>Reported as mg/L calcium carbonate.

<sup>d</sup>Total mg/L.

<sup>e</sup>Not detected.

## RESULTS

### Acidic Waste-Rock Interactions

**Experimental observations** Batch-mixing experiments conducted under low-oxygen conditions in pressure vessels indicated that the acidic waste was either partially or entirely neutralized when mixed with the Mt. Simon Sandstone, Potosi Dolomite, and Proviso Siltstone. The waste was rendered nonhazardous by definition (i.e., the pH of the reacted solution was greater than 2). Under ambient conditions (298°K-0.1 MPa), the pH of the waste increased slightly from 1.9 to 2.6 when mixed with the Mt. Simon Sandstone for 15 days (fig. 2). When temperature and pressure were increased to simulate subsurface environments, the 15-day pH of the solution increased; at 328°K-11.7 MPa, the pH of the waste was 3.8.

The pH of the Potosi-acidic waste ranged from 7.2 to 7.4 after 15 days of contact, and the distribution of pH values did not appear to be related to temperature and pressure (fig. 3). Similarly, the 15-day pH of the Proviso-acidic waste mixtures varied from 6.5 to 7.4, showing no temperature-pressure-dependent trends. In both cases, the neutralization of the acidic waste was fairly rapid; steady-state pH values were attained after approximately 4 to 5 days.

The decrease in the acidity of the waste liquid was paralleled by a concomitant decrease in the oxidation-reduction potential (Eh) of the initially oxidized waste. The Eh of each formation-waste mixture rapidly decreased during the first 3 days of contact (fig. 4), and more reducing conditions were generally associated with an increase in temperature and pressure (fig. 4).

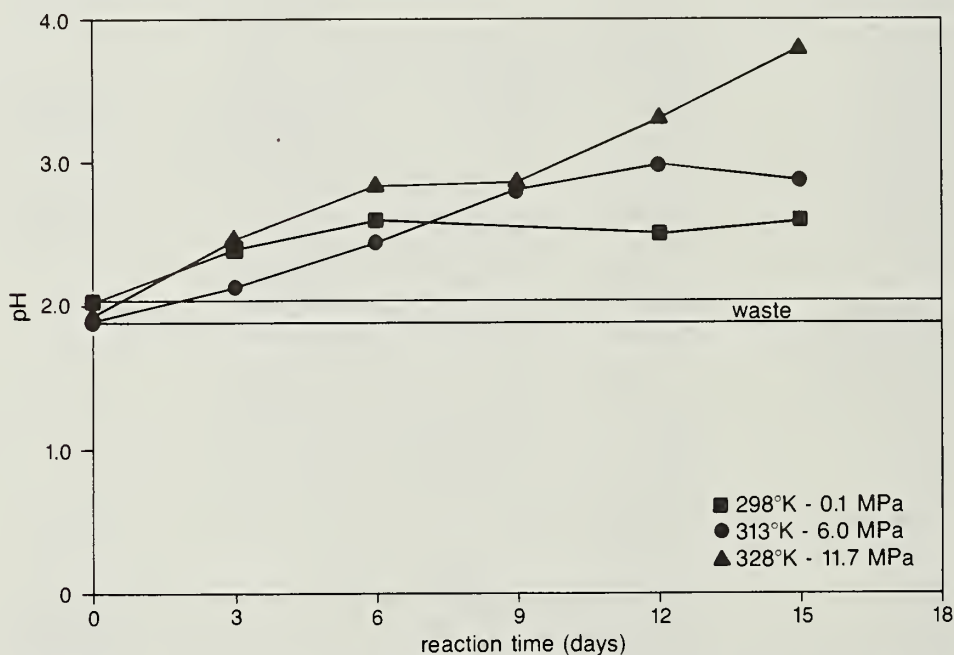


**Figure 2** Change in solution pH of the acidic waste when mixed with the Mt. Simon Sandstone in a closed and low-oxygen system as a function of time, temperature, and pressure (based on a solid-to-liquid ratio of 1:4, wt/vol). Band indicates variation in pH of the waste during the experiments.



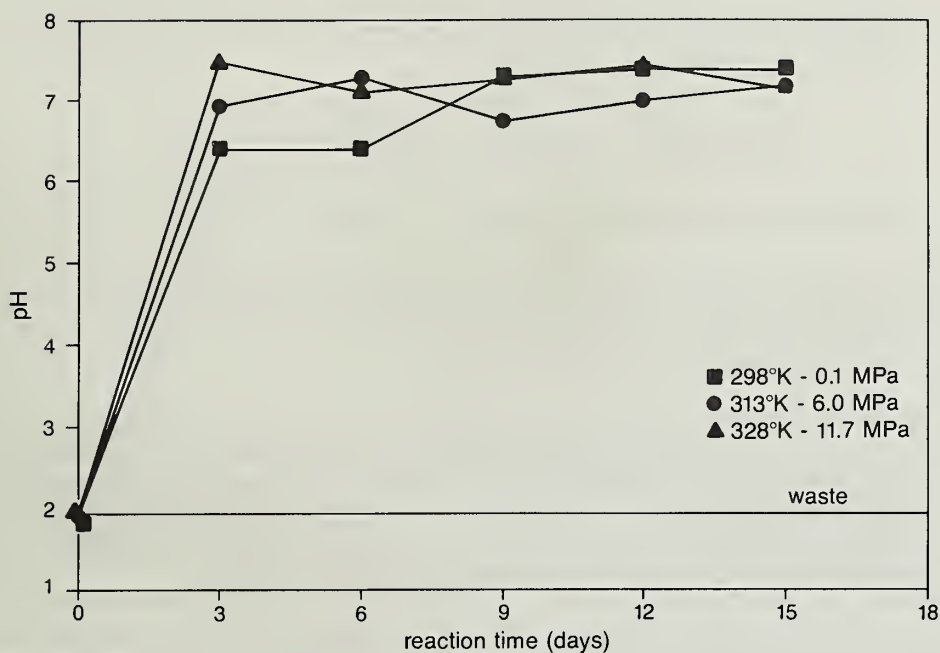


**Figure 3** Change in solution pH of the acidic waste when mixed with the Potosi Dolomite in a closed and low-oxygen system as a function of time, temperature, and pressure (based on a solid-to-liquid ratio of 1:4, wt/vol).

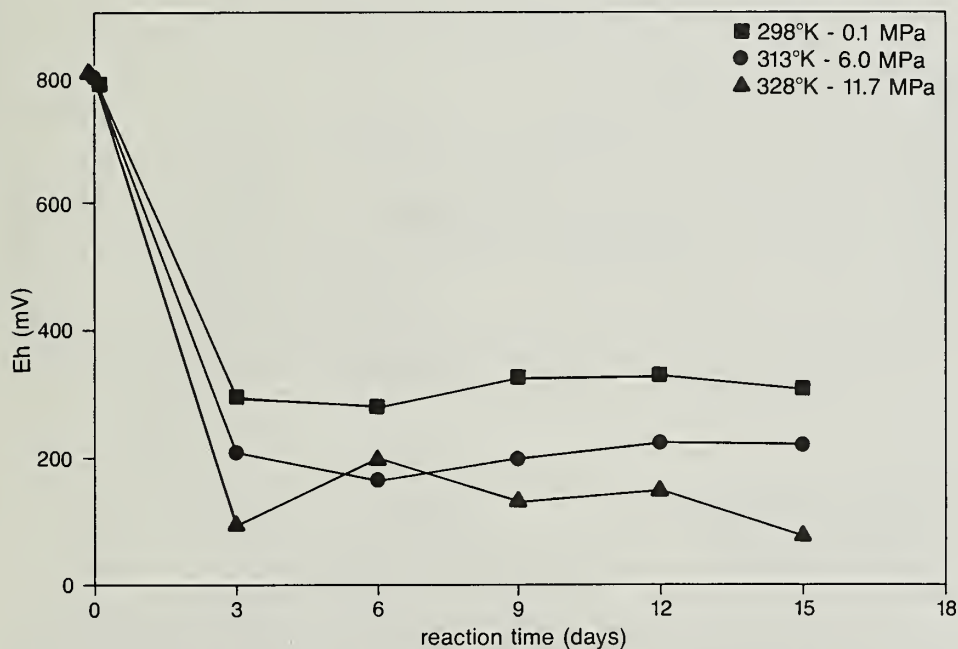
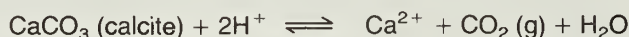


**Figure 4** Change in the oxidation-reduction potential (Eh) of the acidic waste when mixed with the Proviso Siltstone in a closed and low-oxygen system as a function of time, temperature, and pressure (based on a solid-to-liquid ratio of 1:4, wt/vol). All Eh measurements were referenced to a temperature-corrected ZoBell standard.

All three core samples were calcareous to some extent, and the neutralization of the acidic waste produced a concomitant increase in solution Ca (fig. 5) relative to the amount initially present in the waste sample by the reactions:



The Mt. Simon Sandstone sample contained a trace amount of dolomite. Calcium concentrations approached a steady state after 6 to 8 days, and the 15-day Ca concentrations were slightly enhanced at higher temperatures and pressures (fig. 5).

Calcium dissolution was observed in the Potosi-acidic waste and Proviso-acidic waste mixtures, but the dissolution patterns were not strongly correlated with temperature and pressure (fig. 6). The dolomite was composed of approximately 95 percent dolomite, and the degree of Mg in solution (equation 2) increased with an increase in temperature and pressure (fig. 7). The siltstone contained approximately 15 percent dolomite, and the amount of Ca and Mg in solution was comparable to those associated with the Potosi-acid waste mixtures.

When the waste was diluted with an equal volume of a formation brine and mixed with the three cores at 328°K-11.7 MPa, less Ca went into solution (fig. 5). Dilution of acidic wastes with an alkaline brine results in a less acidic solution. A 1:1 dilution of the acidic waste with the brine had a pH of 2.4.

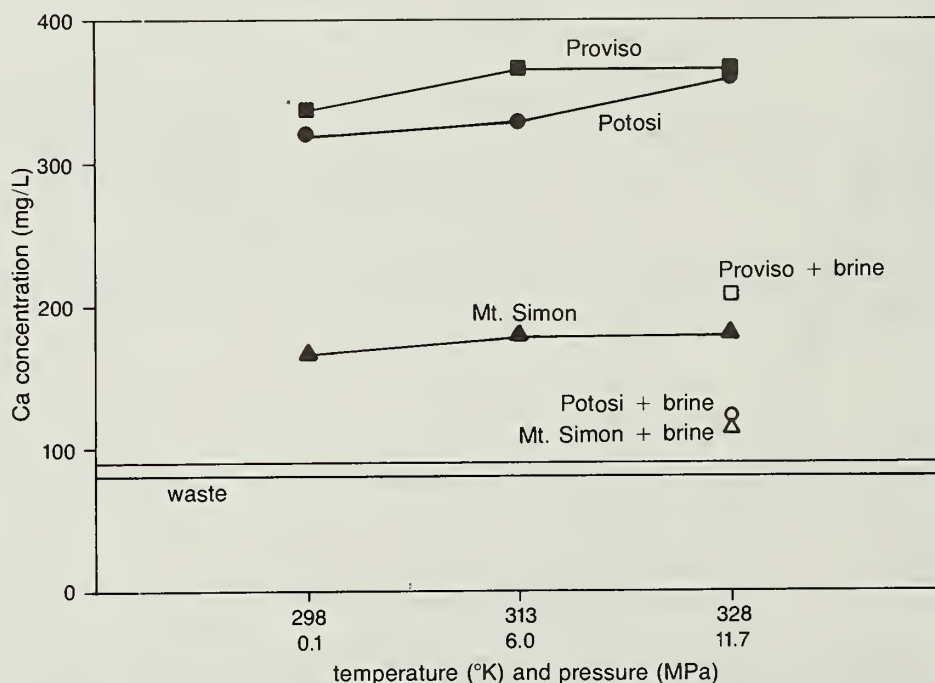


**Figure 5** Concentration of calcium in the acidic waste and waste-brine mixture after 15 days of contact with the Mt. Simon Sandstone, Potosi Dolomite, and Proviso Siltstone in a closed and low-oxygen system as a function of temperature and pressure (based on a solid-to-liquid ratio of 1:4, wt/vol, and a 1:1 dilution with a connate formation brine). Band indicates variation in calcium concentration in the waste during the experiments.

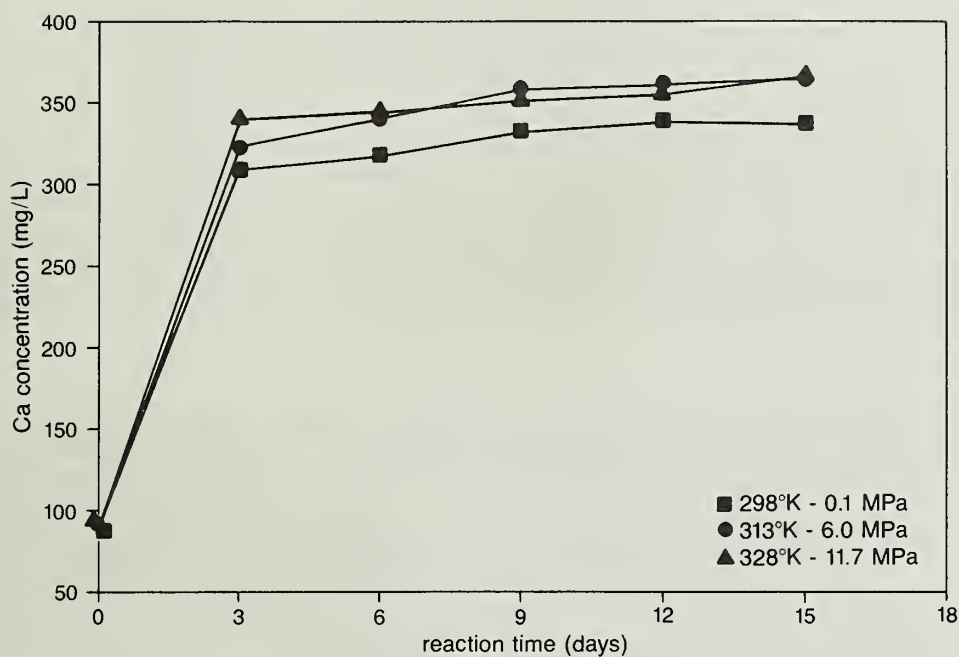


**Figure 6** Change in solution concentration of calcium in the acidic waste when mixed with the Proviso Siltstone in a closed and low-oxygen system as a function of time, temperature, and pressure (based on a solid-to-liquid ratio of 1:4, wt/vol).

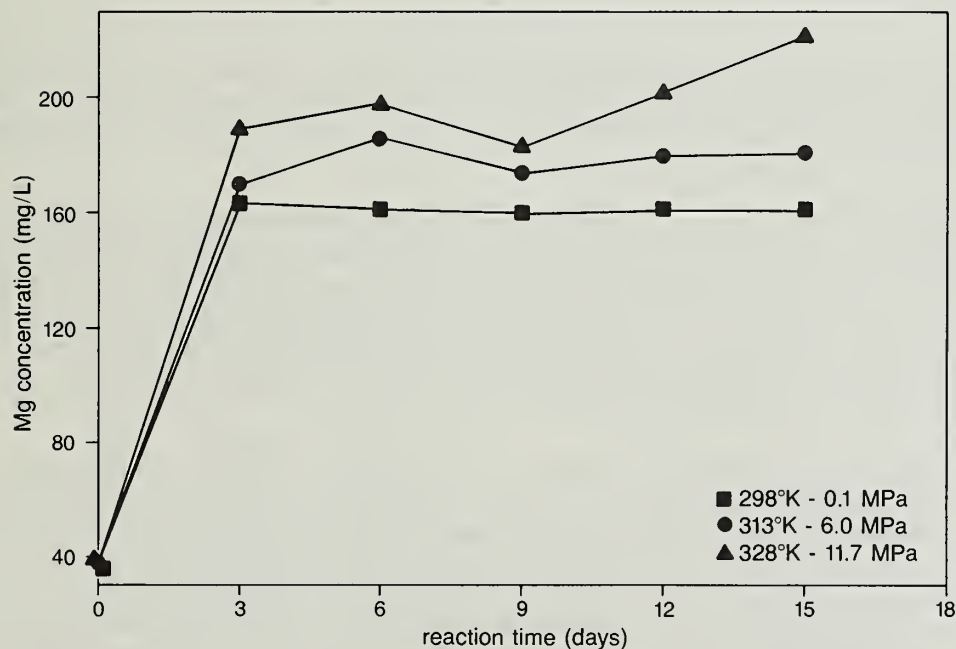


**Figure 7** Change in solution concentration of magnesium in the acidic waste when mixed with the Potosi Dolomite in a closed and low-oxygen system as a function of time, temperature, and pressure (based on a solid-to-liquid ratio of 1:4, wt/vol).



Another indication that carbonate dissolution neutralized the acidic waste was the evolution of gaseous CO<sub>2</sub> (equations 1 and 2). When the head space of the pressure vessel was enriched with CO<sub>2</sub> in all rock-waste systems, the relative amount of CO<sub>2</sub> detected varied. The amount of CO<sub>2</sub> generated within each batch-mixing experiment did not correlate with contact time. Because the rate of waste neutralization was relatively rapid, the concentrations of CO<sub>2</sub> in all of the pressure vessels during the interaction studies were averaged in replicates (table 10). Under ambient conditions, the mean concentrations of CO<sub>2</sub> ranged from 0.72 to 1.8 percent CO<sub>2</sub>. Because of the variability of the data, the individual means were not significantly different from each other at the 95 percent confidence level, based on *t* statistics. The relative amount of CO<sub>2</sub> was reduced by an order of magnitude at the two higher temperatures and pressures (table 10). This reduction was presumably due to the greater gas pressure exerted on the liquid, preventing degassing.

**Table 10** Mean concentration of percent CO<sub>2</sub> in gas samples collected from the head space of reaction vessels after acidic liquid waste was mixed with the core samples during 15-day contact period

Temperature (°K)- pressure (MPa)	Mt. Simon Sandstone <sup>a</sup>	Potosi Dolomite <sup>a</sup>	Proviso Siltstone <sup>a</sup>
Cabot waste only			
298 - 0.1	0.72 ± 0.61	0.84 ± 1.20	1.83 ± 1.47
313 - 6.0	0.05 ± 0.04	0.10 ± 0.03	0.11 ± 0.02
328 - 11.7	0.05 ± 0.01	0.06 ± 0.02	0.07 ± 0.03
Cabot waste and brine			
328 - 11.7	0.04	0.02	0.03

<sup>a</sup>Mean ± 1 standard deviation.

Depending on the pH of the solution, a portion of the dissolved CO<sub>2</sub> was invariably converted to the carbonates H<sub>2</sub>CO<sub>3</sub> and HCO<sub>3</sub><sup>-</sup>. The means given for the nonatmospheric conditions were also not significantly different ( $\alpha = 0.05$ ) from each other. Carbon monoxide and NH<sub>3</sub> were not detected.

The neutralization of the acidic waste may also have been facilitated by the dissolution of aluminosilicate solid phases (fig. 8). The greatest solution of Al was associated with the Mt. Simon Sandstone. The 15-day Mt. Simon acidic waste mixtures were acidic; Al tends to be stable in acidic solutions. In nonacidic systems, such as the 15-day dolomite- and siltstone-acidic waste systems and brine mixtures, Al usually precipitates as aluminum hydroxide. In all three waste-rock systems, an increase in temperature and pressure resulted in slightly lower Al concentrations.

Silica dissolution from the Mt. Simon Sandstone was negligible at 298°K-0.1 MPa pressure (fig. 9). However, when the temperature and pressure of the system were increased to simulate subsurface conditions, silica dissolution was initiated. The initial amount of Si in the acidic waste (6.4 to 7.2 mg Si/L) tended to decrease when mixed with the Potosi Dolomite, but there was no obvious correlation between the amount of silica in solution and temperature. Silica in the Proviso sample was slightly soluble, although like the acidic waste-Potosi systems, there were no apparent temperature-related trends. The degree of silica dissolution in all three waste-rock-brine systems was comparable to that in the absence of the connate brine (see fig. 9). The concentration of Si in the brine (7.87 mg/L) was nearly the same as that in the acidic waste.

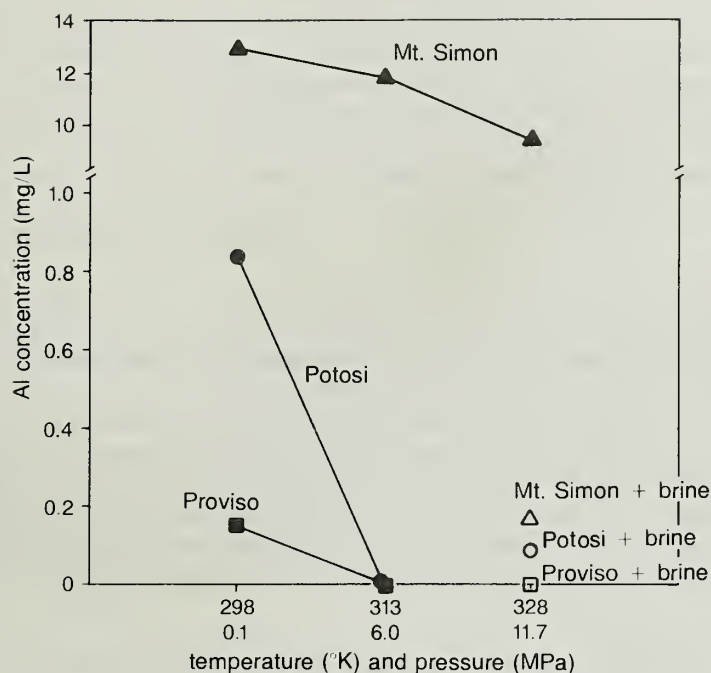


**Figure 8** Concentration of aluminum in the acidic waste after 15 days of contact with the Mt. Simon Sandstone, Potosi Dolomite, and Proviso Siltstone in a closed and low-oxygen system as a function of temperature and pressure (based on a solid-to-liquid ratio of 1:4, wt/vol, and a 1:1 dilution with a connate formation brine).

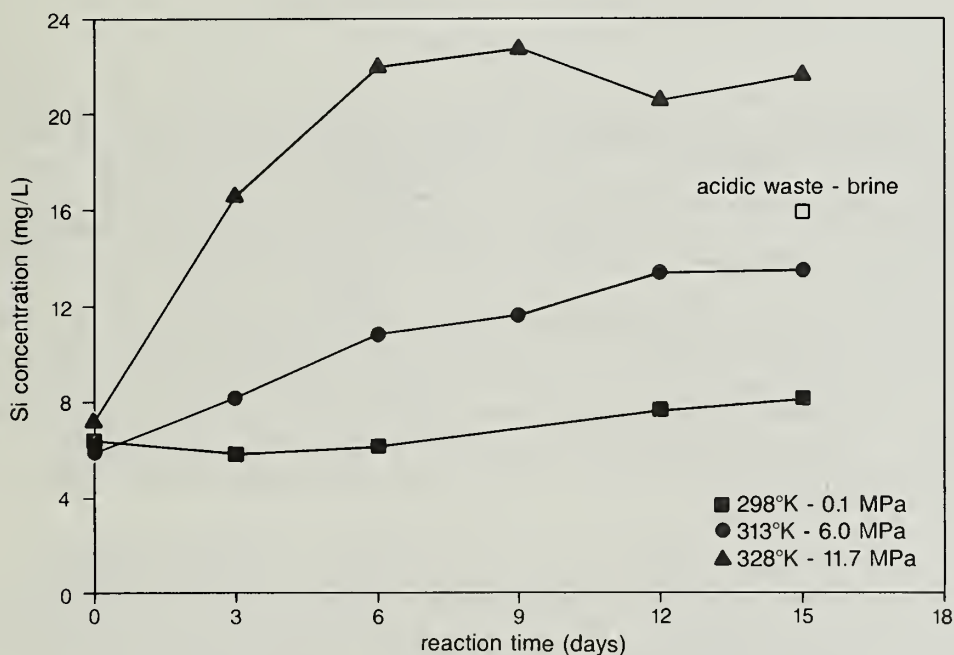
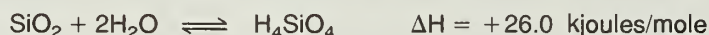


**Figure 9** Solution concentration of silica in the acidic waste and the waste-brine mixture when mixed with the Mt. Simon Sandstone in a closed and low-oxygen system as a function of time, temperature, and pressure (based on a solid-to-liquid ratio of 1:4, wt/vol, and a 1:1 dilution with a connate formation brine).

Heats of reaction were determined under ambient conditions to provide another indicator of chemical reactivity. In general, very little heat was generated by mixing the acidic waste with the three core samples (table 11). Such measurements represent the summation of many exothermic heat producing and endothermic (heat absorbing) reactions that must be interpreted cautiously. The neutralization of HCl by a base (such as  $\text{CaCO}_3$ , equation 1) is an exothermic reaction. Moreover, the dissolution of dolomite and calcite is also exothermic, generating 34.7 and 10.9 kJoules/mole, respectively, whereas the hydrolysis of silica is endothermic,



As discussed previously, the neutralization of the acidic waste was predominantly the result of carbonate dissolution. Since the Potosi Dolomite was essentially a pure dolomite, the neutralization of the waste resulted in the most exothermic reaction of the three core samples (table 11). The Proviso sample contained only 15 percent dolomite that contributed to the exothermicity of the overall reaction, offset by an endothermic contribution of the hydrolysis of quartz. Based entirely on dolomite dissolution, the mean  $\Delta H$  for the siltstone was not proportional to the dolomite content when compared with Potosi. The dissolution of  $\text{CaCO}_3$  would contribute to the exothermicity of the overall reaction, but is not as exothermic as the dissolution of dolomite. Hence, calorimetric data appeared to be in qualitative agreement with experimental observations.

**Table 11** Calorimetric determinations of heats of reaction between the acidic waste and the core samples

Material	$\Delta H$ (joules/g solid at 295°K)
Potosi Dolomite	$-22.8 \pm 1.03$
Proviso Siltstone	$-13.0 \pm 3.01$
Mt. Simon Sandstone	No thermal response

Calorimetric measurements of the Mt. Simon-acidic waste mixtures yielded no detectable thermal response. The previous lines of experimental evidence indicated that the sandstone was the least reactive of the three core samples. At 298°K-0.1 MPa, silica solution was not observed. Therefore, the lack of a thermal response was in agreement with experimental observation. As noted previously, Al dissolution was observed. The lack of a thermal response would also suggest that the appearance of Al in solution was due in part to ion-exchange mechanisms.

**Solubility relationships and reaction mechanisms** The thermodynamic model WATEQ2 (Truesdell and Jones, 1974; Plummer et al., 1976; Ball and Jenne, 1979) was used to help understand the geochemical interactions between the liquid hazardous wastes and the core samples. This computer program is based on the equilibrium constant approach which predicts the distribution of aqueous species based on the input chemical data. The program simultaneously solves several nonlinear equations by successive approximation using the continued fraction approach.

The model WATEQ2 has a temperature range of applicability of 0 to 100°C. Equilibrium constants are calculated at a given temperature using empirical regressions depending on the availability of data for a specific solid phase, or they are interpolated using a van't Hoff equation. This program does not consider pressure-related equilibria. The equilibrium constants for calcite precipitation at 6.0 and 11.7 MPa were calculated from changes in the partial molar volume of the reaction, using the method given in Skirrow (1975). Dolomite equilibria could not be corrected for pressure effects due to a lack of reliable data. The chemical data were also treated by the thermodynamic model SOLMNEQF (Kharaka and Barnes, 1973). SOLMNEQF is similar to



WATEQ2 in terms of structure and database, although fewer solid phases are considered by SOLMNEQF. Like WATEQ2, SOLMNEQF calculates equilibrium constants as a function of temperature using a van't Hoff equation, but it also corrects for pressure over the range from 1 to 1000 atmospheres. Pressure-corrected equilibrium constants of solid phases are approximated using the coefficient of expansion, isothermal compressibility, and molar volume of the mineral phase. The effects of pressure on ionic species are not considered. As with all thermodynamic models, the results must be interpreted cautiously due to discrepancies in reported values for equilibrium constants, heterogeneous redox equilibria, and kinetically inhibited reactions. Both models were used in this study for comparison.

The sandstone-acidic waste system was relatively simple in terms of reaction equilibria. At all temperatures and pressures, the calculated ionic strength varied from 0.036 to 0.040 moles/L showing no time- or temperature-dependent trends. As discussed earlier, the dissolution of dolomite solid phases raised the pH of solution, but not to an extent where carbonate equilibrium was established. The dissolution of feldspars and clay minerals is characteristically a very slow reaction. The relatively slow increase in pH (fig. 2) was interpreted as dissolution reactions with clay minerals rather than as carbonate-mediated neutralization. The only equilibrium relationship indicated by WATEQ2 and SOLMNEQF was the hydrolysis of chalcedony ( $\text{SiO}_2$ ), a fibrous form of quartz (fig. 10). Chalcedony occurs in sedimentary rocks possibly forming from the dissolution of clay minerals (Jenne, 1988). However, for the purposes of this report, chalcedony is presented as a theoretical "model" mineral.

Model calculations indicated that the Si in the waste liquid (fig. 10) was in near equilibrium with chalcedony (approximately 82 percent saturated), which was somewhat consistent with the genesis of the waste, the production of amorphous silica. When the waste was mixed with the sandstone, no quartz dissolution was observed at 298°K (fig. 9), presumably because the solution was already nearly saturated with respect to quartz as chalcedony. At the higher temperatures

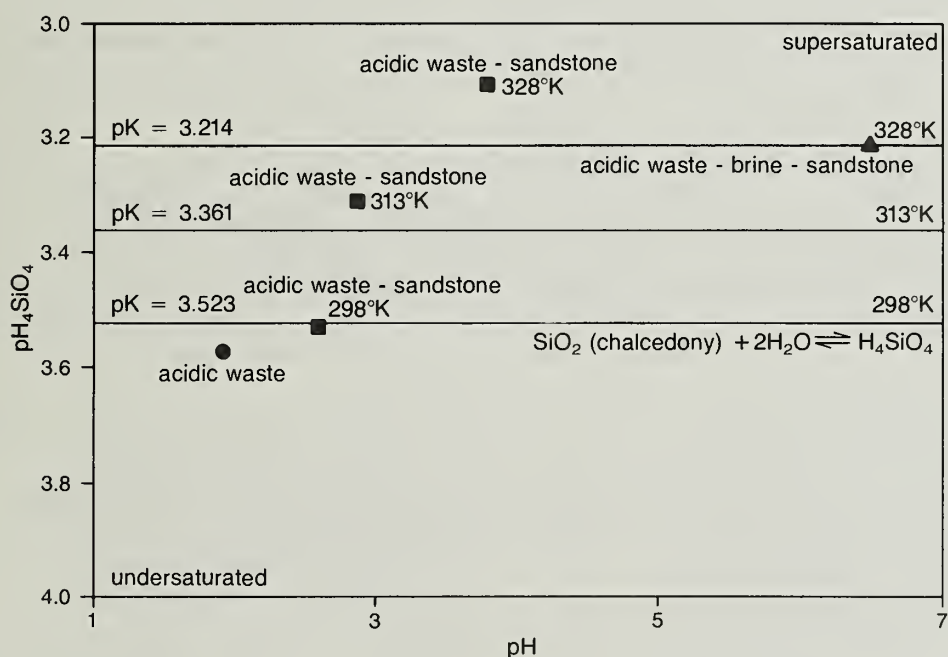


**Figure 10** Silica equilibria of the unreacted acidic waste, waste-Mt. Simon Sandstone mixtures, and the waste-brine-sandstone system after 15 days of solid-liquid contact.

and pressures, the increased dissolution of Si was due to the increased solubility of chalcedony (fig. 10). The waste-brine system also equilibrated with chalcedony. The solution activity of  $\text{H}_4\text{SiO}_4$  was 98.9 percent of that predicted by the solubility of chalcedony at 328°K. Hence, it appeared that the amount of silica in solution in this system could be estimated using equilibrium constants for the hydrolysis of chalcedony. Therefore, this approach could be used in modeling to predict the dissolution of chalcedony in similar deep-well scenarios.

The Potosi-acidic waste system was also relatively simple in terms of reaction equilibria. At all temperatures and pressures, the calculated ionic strength of the solutions varied from 0.046 to 0.054 moles/L, showing no time- or temperature-dependent trends. The acidic waste was neutralized by the dissolution of dolomite. However, dolomite equilibrium was not attained at any temperature. Model results indicated that the solutions were supersaturated (>1000 percent) with respect to a dolomitic carbonate phase. The liquid phase may not have reached equilibrium during the 15-day contact interval. The time required to establish dolomite equilibrium is not known. Attempts to precipitate a dolomitic phase at low temperatures from supersaturated solutions in laboratory situations have been unsuccessful (Stumm and Morgan, 1981). Kinetically, the deposition of magnesium calcite may be more favorable than dolomite, followed by a slow post-depositional conversion to dolomite. Hence, in this case, the extent of formation dissolution could not be accurately predicted by the solubility of a mineral phase known to be present in the core sample.

The dissolution of quartz in the acidic waste-dolomite system was expected. However, the kinetics of quartz dissolution-precipitation at temperatures less than 323°K (50°C) are extremely slow (Stumm and Morgan, 1981). The models indicated that the 15-day solutions had not equilibrated with quartz (fig. 11). In the presence of brine, the thermodynamic activity of  $\text{H}_4\text{SiO}_4$  was approximately 83 percent of that predicted by the solubility of quartz at 328°K.

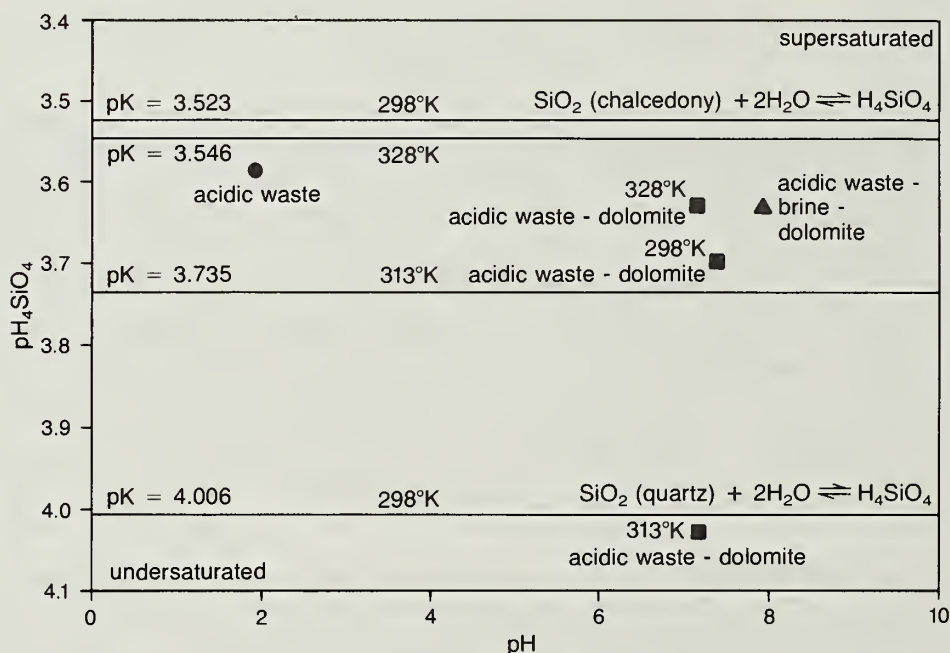


**Figure 11** Silica equilibria of the unreacted acidic waste, waste-Potosi Dolomite mixtures, and the waste-brine-dolomite system after 15 days of solid-liquid contact.



The Proviso-acidic waste system, relative to the other two systems, was more complex. The calculated ionic strength of the solutions ranged from 0.044 to 0.048 moles/L. Feldspar and clay minerals accounted for approximately 35 percent of the solid phases, but like the Mt. Simon Sandstone appeared to exert little influence on the thermodynamic activities of the aqueous species.

As with the Potosi Dolomite, the dissolution of dolomite in the Proviso sample was the most obvious mechanism for the neutralization of the acidic waste. However, model results again indicated that dolomite equilibria was not attained at any temperature and pressure. All solutions, including the brine mixtures, were supersaturated (~2000 percent) with respect to  $\text{CaMg}(\text{CO}_3)_2$ . The same solutions were also supersaturated with respect to calcite. Studies have demonstrated that calcite is more soluble when  $\text{Mg}^{2+}$  is present in solution. The  $\text{Mg}^{2+}$  derived from the dissolution of dolomite could have formed  $\text{Mg-CO}_3$  complexes which would reduce the activity of  $\text{CO}_3^{2-}$  in solution, inducing further calcite dissolution (see Hassett and Jurinak, 1971; Berner, 1975).

The activity of  $\text{H}_4\text{SiO}_4$  in the Proviso-acidic waste system appeared to be controlled by the solubility of chalcedony only at the highest temperature and pressure. At 328°K-11.7 MPa, SOLMNEQF indicated that the activity of  $\text{H}_4\text{SiO}_4$  was approximately 101 percent of that predicted by the solubility of chalcedony. At the lower temperatures, the solutions were slightly supersaturated with respect to chalcedony and quartz. The application of elevated temperature may have accelerated the rate of attainment of equilibrium in the 328°K-11.7 MPa system.

### Alkaline Waste-Rock Interactions

**Experimental observations** Batch-mixing experiments conducted under low-oxygen conditions indicated that the Velsicol hazardous waste did not react strongly with the three core samples. The pH of the liquid phase of the waste-formation mixtures randomly fluctuated between 11.5 and 13.1, and did not appear to correlate with formation type, time, or temperature and pressure. At 298°K-0.1 MPa and 313°K-6.0 MPa, the waste remained hazardous using pH as the hazardous criterion; the pH values were greater than 12.5. At 328°K-11.7 MPa, the waste was nonhazardous by definition (see Appendix A), but remained highly alkaline, ranging in pH from 11.5 to 12.4. In the presence of brine, the pH of the mixtures at 328°K-11.7 MPa varied from 11.9 to 12.0 for all three systems.

Although the Eh the solution remained essentially constant during the batch-mixing studies at 298°K, the solutions tended to become more reduced with time at the elevated temperatures and pressures (see fig. 12). The dissolved oxygen content of the waste at room temperature ranged from 3.9 to 4.9 mg  $\text{O}_2$ /L during the project. At 328°K-11.7 MPa, the concentration of dissolved  $\text{O}_2$  decreased to less than 2 mg  $\text{O}_2$ /L after 15 days of contact. In the presence of the connate brine, the dissolved  $\text{O}_2$  content ranged from 0.8 to 1.5 mg/L in the relatively reduced solutions. However, dissolved oxygen did not correlate with oxidation-reduction (Eh) data.

The alkaline waste was essentially a concentrated salt solution. The experimental observations with respect to chemical interactions were very different from those made with the dilute acidic waste. In terms of calcium solution, the Mt. Simon Sandstone was unreactive with the alkaline waste at 298°K-0.1 MPa, while a minor increase of Ca in solution was detected in the other two waste-rock mixtures (see fig. 13). In each waste-rock system, an increase in temperature and pressure was associated with lower quantities of Ca in solution (fig. 13). As shown in figure 14, the 15-day Ca concentrations at 328°K-11.7 MPa in all three systems were lower than the amount initially present in the waste. This trend also suggested that fate or compatibility-type demonstrations conducted under ambient conditions may not generate data that simulate subsurface conditions.

Unlike the acidic waste-rock systems, the interaction of the alkaline waste with the formation samples resulted in little evolution of gases. At 298°K-0.1 MPa, the mixing of the alkaline waste



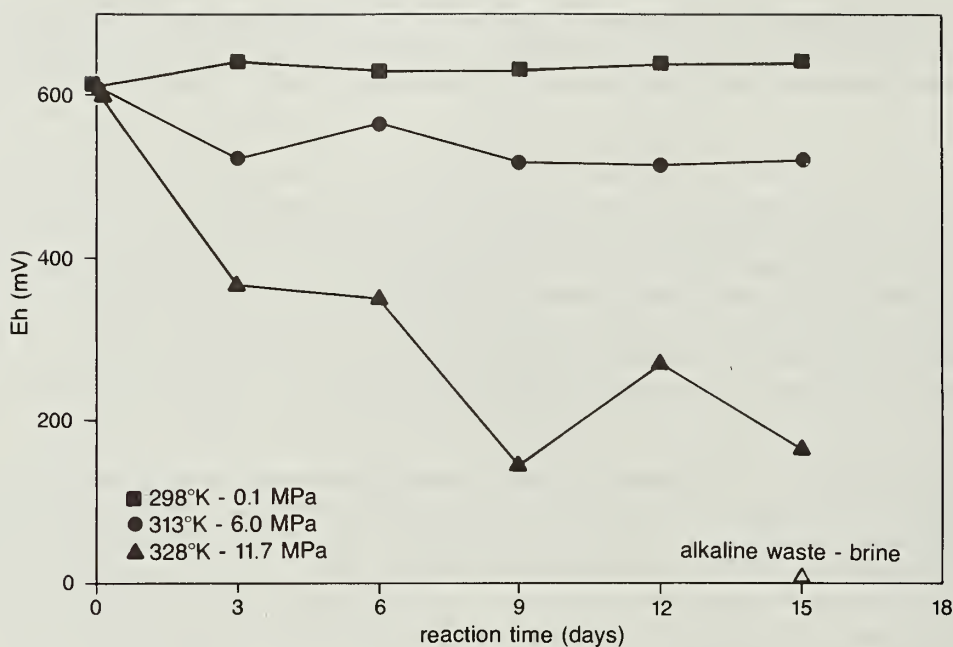


**Figure 12** Oxidation-reduction potential (Eh) of the alkaline waste when mixed with the Proviso Siltstone in a closed and low-oxygen system as a function of time, temperature, and pressure, and a 1:1 dilution with a connate formation brine (based on a solid-to-liquid ratio of 1:4, wt/vol, and a 1:1 dilution with a connate formation brine). All Eh measurements were referenced to a temperature-corrected ZoBell standard.

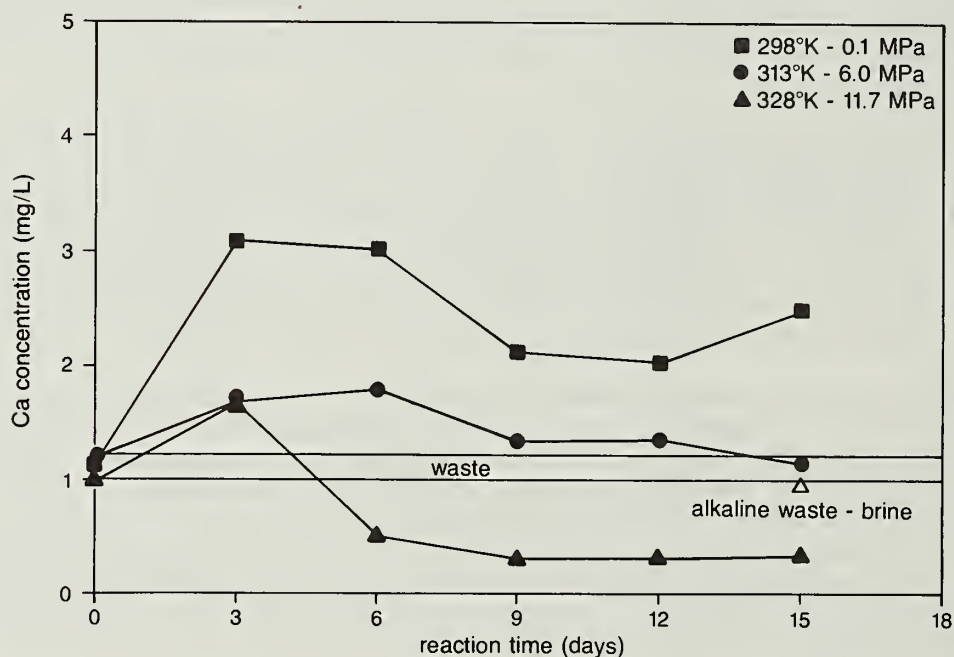


**Figure 13** Solution concentration of calcium in the alkaline waste when mixed with the Potosi Dolomite in a closed and low-oxygen system as a function of time, temperature, and pressure (based on a solid-to-liquid ratio of 1:4, wt/vol, and a 1:1 dilution with a connate formation brine). Band indicates variation in calcium concentration in the waste during the experiments.

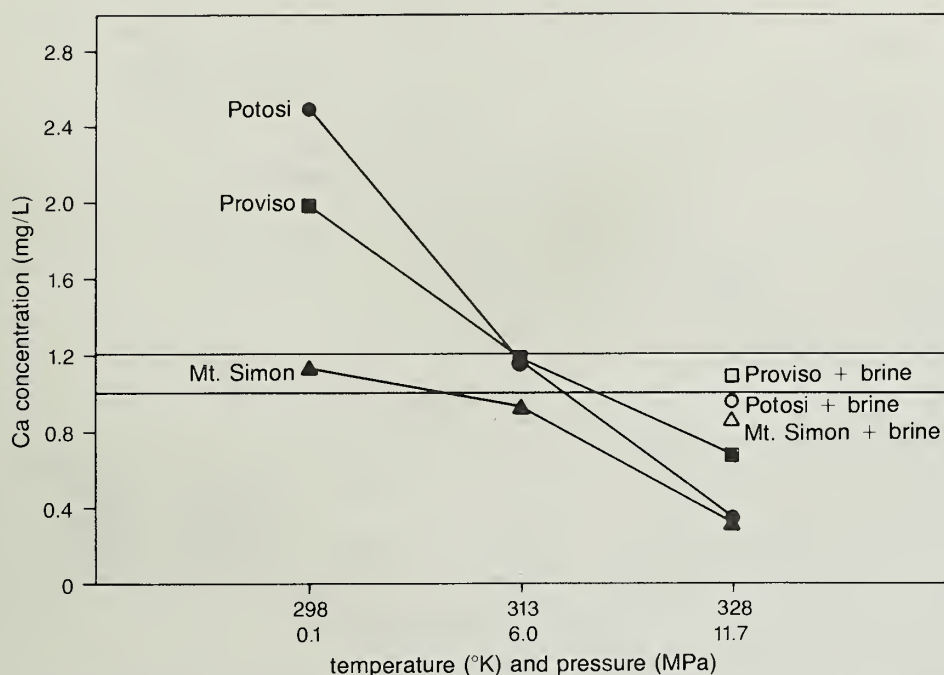


**Figure 14** Concentration of calcium in the alkaline waste and the waste-brine mixture after 15 days of contact with the Mt. Simon Sandstone, Potosi Dolomite, and Proviso Siltstone in a closed and low-oxygen system as a function of temperature and pressure (based on a solid-to-liquid ratio of 1:4, wt/vol, and a 1:1 dilution with a connate formation brine). Band indicates variation in calcium concentration in the waste during the experiments.

with the Potosi Dolomite resulted in approximately 0.02 percent  $\text{CO}_2$ . At higher temperature and pressures, no gas evolution was detected. No gases were detected when the waste was mixed with the sandstone or siltstone at any temperature and pressure.

The dissolution of sulfate was observed in all three systems. Unlike the dissolution behavior of Ca, an increase in temperature and pressure was generally associated with an increase in  $\text{SO}_4^{2-}$  (fig. 15). Sulfate concentrations appeared to be approaching a steady-state relationship toward the end of the 15-day contact interval in all three systems.

Given that the waste was a highly alkaline medium, the Mt. Simon Sandstone was expected to dissolve (fig. 16). An increase in temperature and pressure was associated with a corresponding increase in the amount of Si in solution. The Si dissolution patterns associated with the Proviso Siltstone were similar to those of the sandstone, although it did not appear that steady-state concentrations were attained at the elevated temperatures. At 298°K-0.1 MPa, the siltstone was apparently stable in the alkaline waste (fig. 17).

Quartz was a minor component of the dolomite, and Si dissolution was detected at 298°K-0.1 MPa. With an increase in temperature and pressure, the amount of Si in the waste-dolomite mixtures was approximately the same as that in the unreacted waste (fig. 18). In the presence of brine, the amount of Si in solution was apparently enhanced.

The dissolution of Si was paralleled by the dissolution patterns of Al. Both the Mt. Simon Sandstone and Proviso Siltstone were soluble in terms of releasing Al into solution (fig. 19, for example). At the end of the 15-day contact interval, steady-state concentrations had not been achieved at the elevated temperatures. The Al dissolution patterns of the dolomite-alkaline waste mixture were complex and inconsistent. The amount of Al in solution tended to be less than 0.2 mg Al/L, and decreased at the elevated temperatures.

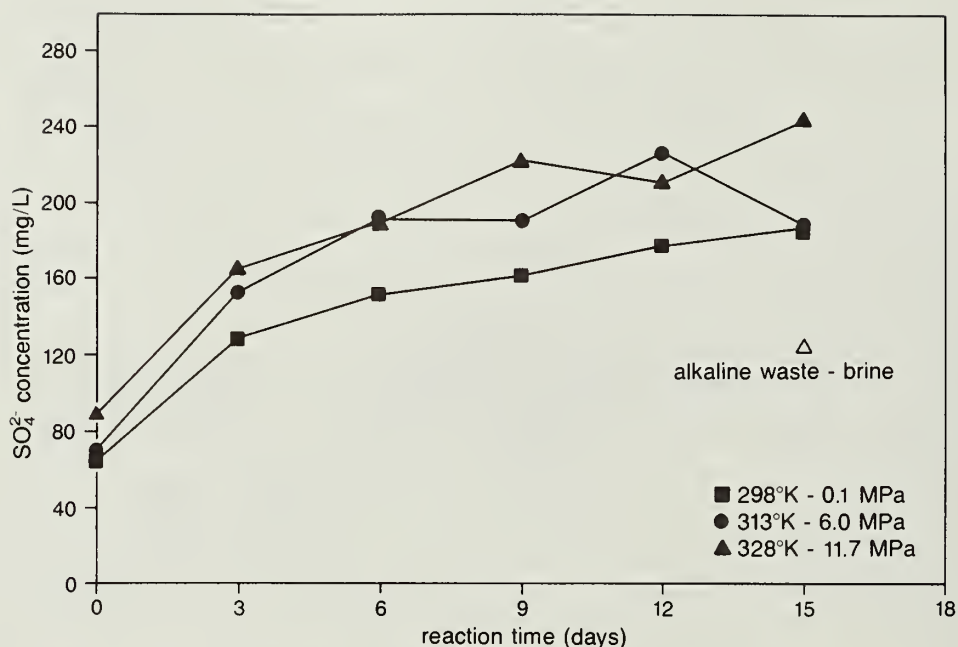


**Figure 15** Solution concentration of sulfate in the alkaline waste and the waste-brine mixture when mixed with the Mt. Simon Sandstone in a closed and low-oxygen system as a function of time, temperature, and pressure (based on a solid-to-liquid ratio of 1:4, wt/vol, and a 1:1 dilution with a connate formation brine).

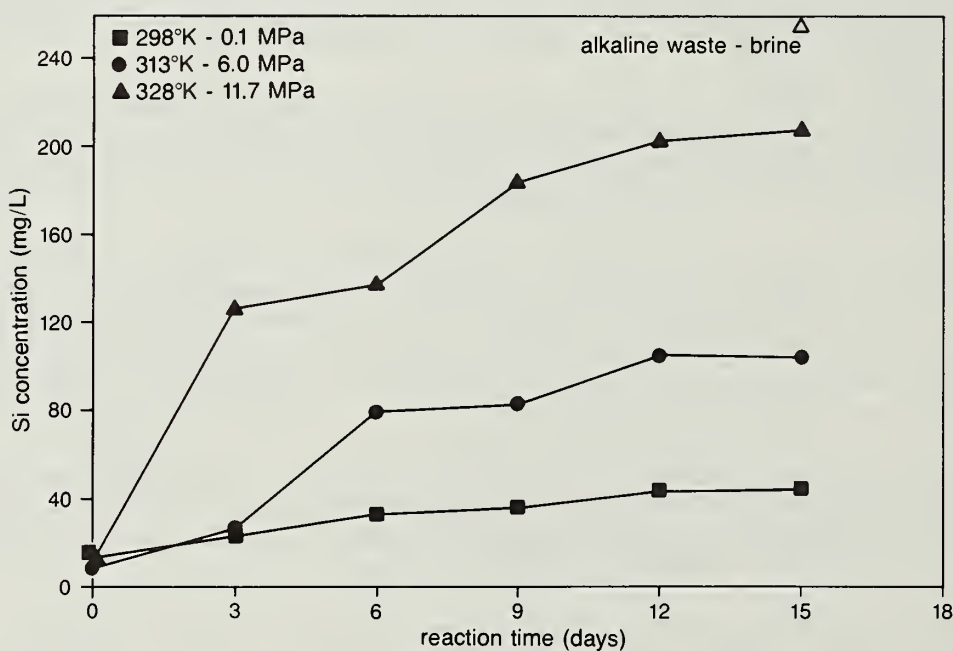


**Figure 16** Solution concentration of silica in the alkaline waste and the waste-brine mixture when mixed with the Mt. Simon Sandstone in a closed and low-oxygen system as a function of time, temperature, and pressure (based on a solid-to-liquid ratio of 1:4, wt/vol, and a 1:1 dilution with a connate formation brine).



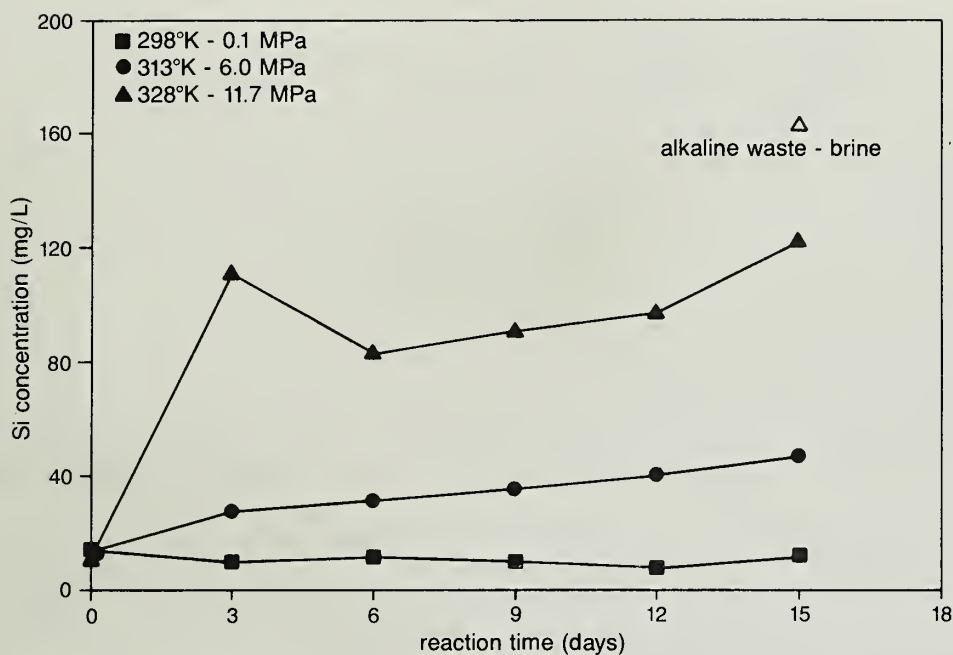


**Figure 17** Solution concentration of silica in the alkaline waste and the waste-brine mixture when mixed with the Proviso Siltstone in a closed and low-oxygen system as a function of time, temperature, and pressure (based on a solid-to-liquid ratio of 1:4, wt/vol, and a 1:1 dilution with a formation brine).

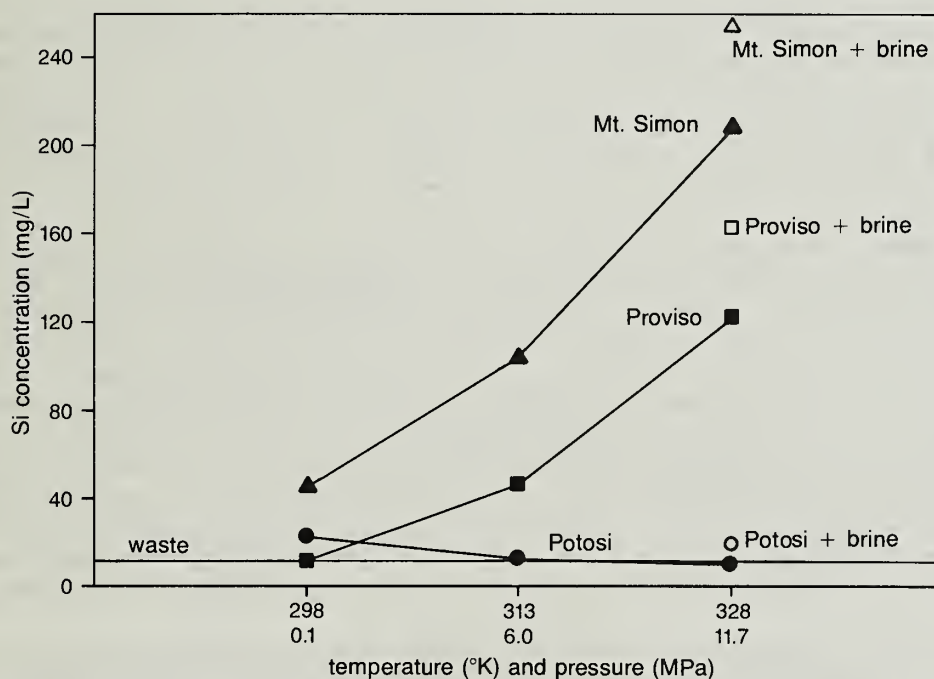


**Figure 18** Concentration of silica in the alkaline waste and waste-brine mixture after 15 days of contact with the Mt. Simon Sandstone, Potosi Dolomite, and Proviso Siltstone in a closed and low-oxygen system as a function of temperature and pressure (based on a solid-to-liquid ratio of 1:4, wt/vol, and a 1:1 dilution with connate formation brine).

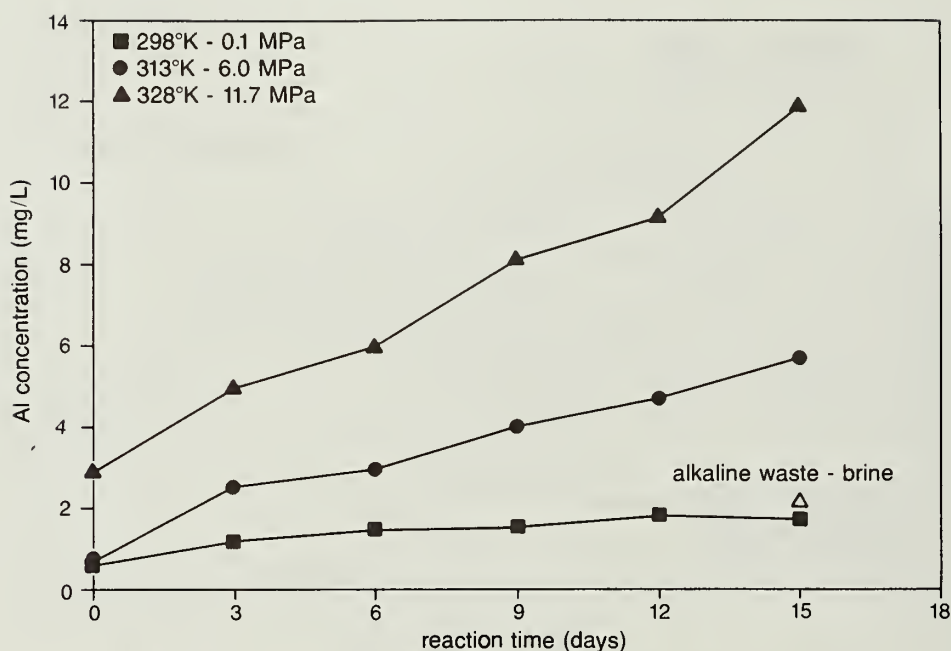


**Figure 19** Solution concentration of aluminum in the alkaline waste after 15 days of contact with the Mt. Simon Sandstone in a closed and low-oxygen system as a function of temperature and pressure (based on a solid-to-liquid ratio of 1:4, wt/vol, and a 1:1 dilution with connate formation brine).

The laboratory data generally indicated that the alkaline waste did not react strongly with the formations with the exception of the dissolution of silicates. Mixing the waste with the core samples at room temperature did not yield detectable changes in heat content by calorimetry. All heats of reaction measurements were below detection ( $\pm 3.6$  joules/g). The hydration of quartz is an endothermic reaction, which may have been cancelled by the contribution of exothermic reactions of similar magnitude. As noted earlier, chemical reactivity (figs. 16-19) tended to be minimal under ambient conditions, i.e., under the conditions at which the calorimetry was applied.

**Solubility relationships and reaction mechanisms** The chemical data from the batch-mixing experiments were also treated by the thermodynamic models WATEQ2 and SOLMNEQF. However, only limited interpretations of the results were attempted because of the high ionic strength of the alkaline waste. Nordstrom and Ball (1984) concluded that ion-association models (such as WATEQ2 and SOLMNEQF) cannot be used to predict mineral solubilities or solute activities at ionic strengths exceeding 0.6 moles/L. The methods and concepts used by these programs, such as the estimation of activity coefficients, were based on solutions with much lower ionic strengths than that of the alkaline waste, which had a calculated ionic strength of approximately 4.6 moles/L. Consequently, the waste sample was beyond the range at which reliable data are available for ion associations and hydrolytic reactions for some reactions. Recent advances have resulted in models that are applicable to high-ionic strength solutions (Crowe and Longstaffe, 1987), but these models were unavailable when this investigation was conducted.

The model results suggested that the alkaline brine-like waste was undersaturated with respect to halite; the calculated ion activity product was 31 percent of the solubility of halite at 295°K. Salt crystals formed in discarded samples of the waste in approximately one week as the solutions evaporated. The waste was apparently undersaturated with respect to  $\text{SiO}_2$  and was not in equilibrium with any solid phase considered by WATEQ2.

According to the models, the alkaline waste-Mt. Simon system was supersaturated with respect to calcite at 298°K-0.1 MPa, but may have been approaching calcite equilibrium at 313°K-11.7 MPa after 12 to 15 days of contact (fig. 20). The WATEQ2-calculated ion activity product of the 15-day, 328°K-11.7 MPa solution was approximately 97 percent of the solubility of  $\text{CaCO}_3$  when corrected for both temperature and pressure. The waste-brine-sandstone system also appeared to have attained calcite equilibrium; the solution was approximately 78 percent of the solubility of calcite. The chemical composition of this system implied interaction between the waste and the connate formation brine. The waste contained approximately 1 mg Ca/L, whereas the brine had 147 mg Ca/L. When the two liquids were mixed, the solution concentration of Ca was less than 1 mg/L, suggesting that Ca precipitated. When the waste was mixed with brine in a beaker in the laboratory, a white precipitate formed in a matter of minutes. The precipitate was analyzed by X-ray diffraction, but no crystalline phases other than halite and sylvite (KCl) were detected in dried samples. While X-ray diffraction was no assistance, the chemical model supported this visual observation by suggesting the attainment of  $\text{CaCO}_3$  equilibrium. Hence, it would appear that the initial injection of the alkaline waste could precipitate a carbonate phase by reacting with the formation waters, given the excess of carbonate ions in the waste.

The connate brine sample also contained 117 mg/L magnesium (table 8) that disappeared from solution when mixed with the brine. Circumstantial evidence indicated that it precipitated as brucite ( $\text{Mg}(\text{OH})_2$ ). In an unrelated study, Mehnert et al. (1988) found that brucite precipitated near the injection zone at the Velsicol facility at Marshall, Illinois. In this study, equilibrium modeling indicated that a Mg concentration in excess of approximately 0.1  $\mu\text{g/L}$  in the waste-brine mixture would result in a supersaturated solution with respect to brucite. The analytical detection limit for Mg was 0.07 mg/L (table 2), which precluded assessing brucite equilibria. The inability to determine very low solution concentrations (such as Mg) is a limitation in using equilibrium models coupled with laboratory studies to predict chemical interactions. On the basis of the argument

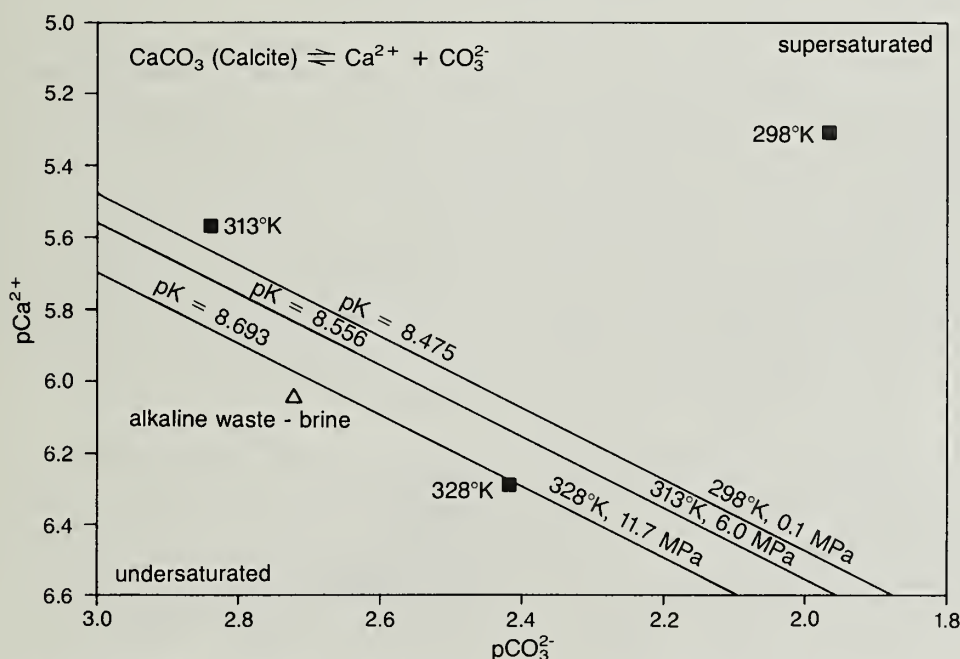


**Figure 20** Calcite equilibria of the alkaline waste-Mt. Simon Sandstone mixtures and the waste-brine-sandstone system after 15 days of solid-liquid contact.



above, the white precipitate that formed when the waste was mixed with brine probably contained a magnesium hydroxide phase in addition to calcium carbonate.

The Potosi-alkaline waste system was also supersaturated with respect to calcite at 298°K-0.1 MPa, but as temperature and pressure were increased, the system appeared to be approaching calcite equilibrium from the supersaturated field (fig. 21). The presence of organic compounds adsorbed on solid surfaces (such as those listed in tables 4, 5, and 6) could retard the rate of calcite crystallization (Skirrow, 1975). Skirrow generalized that rapid  $\text{CaCO}_3$  precipitation from seawater does not occur until much of the dissolved organic matter is removed. The major organic compound in the alkaline waste, hexachlorocyclopentadiene, can be adsorbed by clay minerals (see Chou and Griffin, 1983). Consequently, the organic solutes in the alkaline waste may have retarded the development of calcite equilibrium.

The Proviso-alkaline waste were also supersaturated with respect to calcite according to the model. With an increase in temperature and pressure the degree of saturation tended to decrease, although the least saturated solution (12 day, 328°K-11.7 MPa) was still approximately 156 to 275 percent of the solubility of crystalline calcite. As discussed earlier, plausible mechanisms exist that could delay the development of well-defined mineral equilibria. As noted earlier (fig. 14), the concentration of Ca in solution decreased with an increase in the temperature and pressure of the system. The solubility of calcite decreases with temperature, and increases with pressure, although temperature dominates. Hence, the influence of calcite solubility was a probable reaction mechanism controlling the activity of  $\text{Ca}^{2+}$ .

The solution patterns of sulfate in all three systems could not be clearly attributed to the solubility of gypsum ( $\text{CaSO}_4 \cdot 2\text{H}_2\text{O}$ ), the most probable source of  $\text{SO}_4^{2-}$ . Gypsum was not detected in the core samples by X-ray diffraction. The solubility of gypsum increases in the 298 to 328°K temperature range, as did sulfate concentrations. However, WATEQ2 and SOLMNEQF modeling

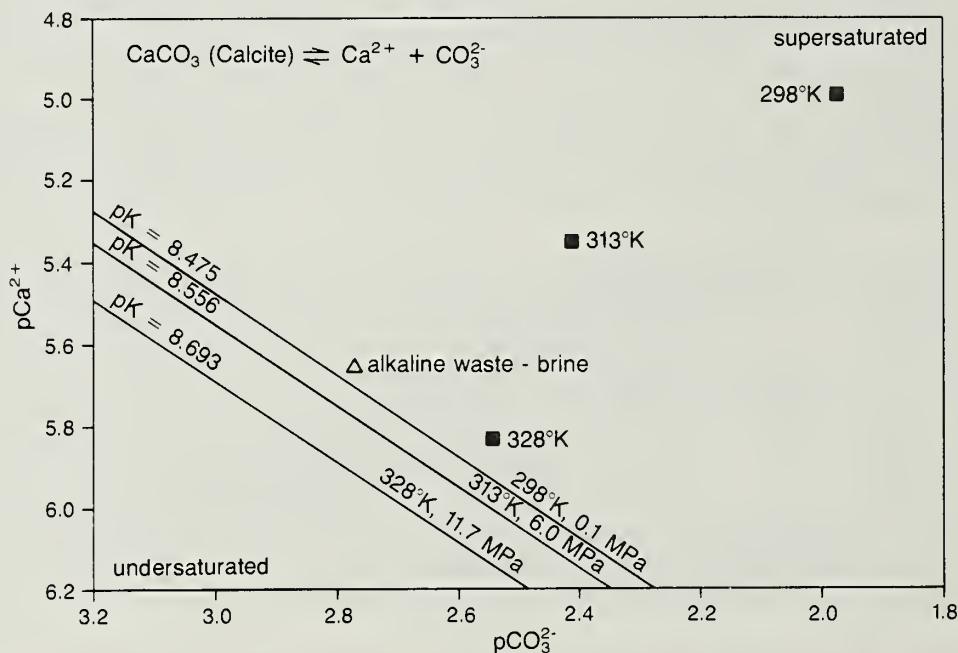


**Figure 21** Calcite equilibria of the alkaline waste-Potosi Dolomite mixtures and the waste-brine-dolomite system after 15 days of solid-liquid contact.

results indicated that ion activity products of  $\text{Ca}^{2+}$  and  $\text{SO}_4^{2-}$  never exceed 0.003 percent of the solubility of gypsum at any temperature. The solutions were also undersaturated with respect to anhydrite ( $\text{CaSO}_4$ ). The concentrations of Ba and Mg were below analytical detection limits (typically less than 0.07 mg/L), which precluded assessing if barite ( $\text{BaSO}_4$ ) or other minerals were possible sources of sulfate. The Proviso Siltstone sample contained pyrite ( $\text{FeS}_2$ ) at the top of the sampled interval (see Appendix C, table C2) that could have oxidized yielding sulfate. Pyrite was not observed in the other two core intervals. The sulfate equilibria of the core alkaline waste systems remained unresolved.

The Si solubility mechanisms were also investigated. The models WATEQ2 and SOLMNEQF indicated that all of the waste mixtures were undersaturated with respect to quartz and amorphous  $\text{SiO}_2$ . Batch-mixing data such as figures 16 and 17 suggested that in some cases, Si had not reached a steady state. Little silica dissolved from the Proviso Siltstone in the alkaline waste at 298°K-0.1 MPa. However, model results suggested that the activity of Si in the system was at most 0.21 percent of the solubility of quartz. Because the solutions were undersaturated with respect to quartz, solution thermodynamics dictates that quartz should dissolve. The solubility of quartz is greater in alkaline (pH >10) media, such as this waste, than in acidic media. In the presence of brine, all three systems were vastly undersaturated with respect to quartz (<0.5 percent) according to WATEQ2 and SOLMNEQF.

## CONCLUSIONS

The chemical reactivity of two hazardous wastes, a dilute acidic liquid, and an alkaline concentrated brine-like solution, with injection-zone materials was investigated by conducting laboratory studies. The liquid wastes were mixed with disaggregated-core samples of the Mt. Simon Sandstone, Potosi Dolomite, and the Proviso Siltstone under low-oxygen conditions in pressure vessels that were simultaneously heated and pressurized to simulate subsurface conditions. Batch-mixing experiments were conducted for 15 days at three temperatures and pressures (298°K-0.1 MPa, 313°K-6.0 MPa, and 328°K-11.7 MPa). Additional experiments were conducted by diluting the wastes with a connate formation brine to simulate the mixing zone in an injection scenario.

### Waste Interactions with the Mt. Simon Sandstone

Under the laboratory conditions described, the acidic waste was partially neutralized with up to 15 days of contact. The waste was rendered nonhazardous by pH criterion (i.e., the pH of the reacted solution was greater than 2), but remained acidic. The dominant mechanism of neutralization was the dissolution of clay minerals and ion exchange augmented by the dissolution of a minor amount of calcareous material. The extent of the reaction progressed slightly with an increase in temperature and pressure. The reaction(s) resulted in the evolution of  $\text{CO}_2$  gas, but the gas was not detected at the elevated pressures. The solution activity of silica appeared to be controlled by the thermodynamic solubility of  $\text{SiO}_2$  as chalcedony in both the presence of a connate brine, and in the waste-sandstone mixture. An increase in temperature increased the amount of Si in solution because the solubility of  $\text{SiO}_2$  increases with temperature.

If the acidic waste was injected into the Mt. Simon Sandstone, it would be initially diluted by formation water. If these in situ brines were alkaline, the resulting mixture would be less aggressive to the sandstone. Once the brine becomes displaced near the well, the waste would be further neutralized to an extent governed by the amount of carbonate and clay minerals present. On the basis of chemical considerations, sandstone porosity would not appear to be significantly altered by the dissolution of solid phases, or by the exsolution of a separate gas phase. However, porosity measurements per se were not made.

The alkaline waste reacted with the Mt. Simon Sandstone, but remained hazardous at the two lower temperatures and pressures; the pH of the waste remained above 12.5. At 328°K-11.7 MPa, the waste was rendered nonhazardous by pH criterion in that the pH of the waste was less than 12.5. However, the pH values of the solutions were still very alkaline, ranging from 11.5 to



12.4. The solution activity of  $\text{Ca}^{2+}$  may have been controlled by the thermodynamic solubility of calcite. When the waste was mixed with the connate brine in a 1:1 (vol:vol) ratio, the excess of  $\text{CO}_3^{2-}$  probably precipitated  $\text{CaCO}_3$ . This reaction would be more likely with an increase of injection depth because the solubility of calcite decreases with increasing temperature.

On the basis of the amount of silica in solution, approximately 0.2 percent of the sandstone dissolved in the alkaline waste after 15 days of contact at 328K-11.7 MPa. The solutions did not appear to attain steady state with any solid silica mineral considered by the models WATEQ2 and SOLMNEQF. The reactions between the waste and sandstone yielded no detectable evolution of gases or heat.

These laboratory data suggested that if the undiluted alkaline waste was injected into the Mt. Simon Sandstone, two major reactions could result. Initially, the waste would react with the formation waters and precipitate carbonate phases and possibly solid magnesium hydroxide. Solubility modeling indicated that the waste-brine sandstone mixture was in equilibrium with calcite. With time, the alkaline waste would probably begin to dissolve the sandstone. The dissolution of the silicates could increase the porosity of the injection zone, leading to the use of lower injection pressures. However, increases in formation porosity could be offset by the precipitation of calcite and brucite on the quartz grains.

It is difficult to predict which of the two processes would predominate without conducting laboratory porosity measurements with core samples. Batch-interaction studies can identify potential problems stemming from chemical interactions. Formation porosity is a physical phenomenon requiring an apparatus or experimental approach to specifically measure porosity. It may be that where calcium carbonate or magnesium hydroxide precipitation is a problem, an alkaline waste would need to be diluted or acidified (e.g., co-disposal with acidic wastes) so that the subsurface brine-waste mixture is undersaturated with respect to calcium carbonate and/or hydroxide. Answering these types of questions is a potential role of batch-interaction studies in the permitting process.

#### **Waste Interactions with the Potosi Dolomite**

Under the laboratory conditions described, the acidic waste was neutralized by the Potosi Dolomite via the dissolution of  $\text{CaMg}(\text{CO}_3)_2$ . The neutralization of the acidic waste appeared to be complete after approximately 4 days of contact, but the distribution of pH values did not correlate with the temperature and pressure of these systems. As expected, the dissolution reaction resulted in the evolution of  $\text{CO}_2$  gas, but the gas was not detected at the elevated pressures and pH. The neutralization of the acidic waste was exothermic, and thus a small temperature increase was detected by calorimetry under ambient conditions. Because the Cabot waste contained only 0.09 weight percent HCl, the temperature increase was negligible. On the basis of thermochemical calculations, temperature increases can become significant ( $>10^\circ\text{C}$ ) when the amount of HCl is greater than approximately 8 percent (see Panagiotopoulos and Reid, 1986).

Although the formation sample was approximately 95 percent dolomite, dolomite equilibrium was not attained at any pressure and temperature under these conditions; the liquid phase was supersaturated with respect to this carbonate phase. Hence, this reaction could not be accurately modeled by the thermodynamic principles of mineral dissolution-precipitation. The solution activity of silica appeared to be influenced by the solubility of quartz, both in the presence of a connate brine and in the waste-dolomite mixtures.

The injection of waste acids, particularly inorganic acids in carbonate formations, has been widely practiced for years and the chemical interactions in such systems have been considered (Kamath and Salazar, 1986). The practice has the obvious attraction of neutralizing a hazardous waste via acid-base chemistry, and the process may increase the capacity of the formation to receive injected wastes. A major concern in this type of system is the occurrence of "well blowout," where the excessive accumulation of gaseous  $\text{CO}_2$  escapes to the surface. The Cabot



Corporation initially injected a 32 percent HCl solution, and in 1975 the well erupted. The amount of CO<sub>2</sub> in solution was far in excess of its solubility in solution at that concentration of HCl. Since the 1975 incident, the Cabot Corporation reduced the concentration of HCl to avoid this problem. The dilute nature of the sample used in this project reflected this concern. No further problems with well blowout have been reported, nor would they be expected based on these laboratory results.

The alkaline waste did not react strongly with the Potosi Dolomite relative to the acidic waste. As with the Mt. Simon Sandstone, the waste remained hazardous after reacting with the dolomite at the lower two temperatures and pressures, but was nonhazardous at 328°K-11.7 MPa using pH (and only pH) as a hazardous criterion. The mixing of the two materials resulted in a small quantity of CO<sub>2</sub> gas, but at the elevated temperatures and pressures the CO<sub>2</sub> was not detected. No detectable heat was absorbed or released during contact between the dolomite and the alkaline waste. The solution activity of Ca<sup>2+</sup> appeared to be influenced by the solubility of calcite, but the relationship was not clear. The amount of total calcium in solution decreased with an increase in temperature and pressure. Sulfate dissolution increased with temperature and pressure, but this trend could not be linked to the thermal stability of a solid sulfate phase. A minor amount of silica dissolution was detected, but only under ambient conditions. At elevated temperatures and pressures, the amount of silica in solution was comparable to that in the waste, suggesting that the quartz did not dissolve significantly under these conditions. However, thermodynamic modeling indicated that the solution was undersaturated with respect to all silicate phases, suggesting that quartz should dissolve. The lack of equilibrium was probably the result of slow-reaction kinetics. This enigma remains unresolved. In the presence of a brine connate, silica dissolution was observed but could not be attributed to the solubility of a particular SiO<sub>2</sub> phase.

#### **Waste Interactions with the Proviso Siltstone**

Under the laboratory conditions described, the acidic waste reacted with the Proviso Siltstone by chemical mechanisms similar to those observed with the Potosi Dolomite. The mixing of the acidic waste with the siltstone represented a worst-case situation--unreacted acid in contact with a confining-layer material. In such a situation, the neutralization of the waste by carbonate phases in the injection zone, and dilution by formation waters before the waste arrives at the cap rock have not been taken into account.

The acidic waste was neutralized by the dissolution of carbonate phases, predominantly dolomite, and the reaction appeared to be complete after 6 days of contact. The distribution of pH values did not correlate with the temperature and pressure of the system. Like the acidic waste-Potosi system, the reaction resulted in CO<sub>2</sub> evolution, but the solution phase was undersaturated with respect to CO<sub>2</sub> at the elevated temperature and pressures. The mixing of the two materials resulted in the evolution of heat, but because of the low concentration of HCl, the resulting temperature increase would be negligible in an injection zone. The sample was composed of 15 percent dolomite, but thermodynamic modeling indicated that the solution did not attain dolomite equilibrium within a 15-day contact period. The solubility of dolomite decreases with temperature; thus, the extent of dissolution would be expected to decrease with depth. In the presence of brine, the solution was supersaturated with respect to both dolomite and calcite; no definable carbonate equilibrium was established. The solution behavior of silica in the waste-Proviso mixtures appeared to be controlled by the solubility of chalcedony, but only at the highest temperature and pressure. The solutions may not have had sufficient time to equilibrate at the lower temperatures.

The alkaline waste also reacted with the siltstone, but as in the other two formations, the waste remained hazardous after direct contact with the disaggregated sample at the two lower temperatures and pressures. At 328°K-11.7 MPa, the waste remained highly alkaline. The mixing of the alkaline waste with the siltstone did not result in the evolution of detectable gases or temperature changes. While the siltstone sample contained about 15 percent dolomite, Mg dissolution was not

detected. The solutions were supersaturated with respect to calcite, but  $\text{Ca}^{2+}$  activity appeared to be influenced to some extent by the solubility of  $\text{CaCO}_3$ . Well-defined carbonate equilibrium could not be resolved.

Little silica dissolved from the siltstone in the alkaline solution under ambient conditions. However, with an increase in temperature and pressure, the amount of silica in solution increased. This experimental observation could not be linked to the thermal stability of any solid silicate phase. When the waste was diluted with brine and mixed with the siltstone at  $328^\circ\text{K}$ -11.7 MPa, the amount of silica in solution translated to approximately 0.3 percent dissolution of the solid mass after 15 days of contact. Hence, these data indicate that siltstone would be dissolved more by alkaline waste than by inorganic acid. It is unknown whether the dissolution of the siltstone in an actual deep-well situation would lead to the migration of alkaline waste from an injection zone.



## REFERENCES

- American Public Health Association. 1975. Standard methods for the examination of water and wastewater (14 ed.). American Public Health Association, Washington, DC., 1193 pp.
- Ball, J. W., and E. A. Jenne. 1979. WATEQ2 - A chemical model for trace and major element speciation and mineral equilibria of natural waters: American Chemical Society Symposium Series 93, Chemical Modeling in Aqueous Systems, p. 815-836.
- Barnes, I. 1972. Water-mineral reactions related to potential fluid-injection problems, in T. D. Cook (ed.), *Underground waste management and environmental implications*. American Association of Petroleum Geologists, Memoir 18, p. 294-297.
- Bayazeed, A. F., and E. C. Donaldson. 1971. Deep-well disposal of steel pickling acid, paper presented (number SPE 3615) at the 46th Annual Meeting of the Society of Petroleum Engineers of AIME, New Orleans, LA, 3-6 Oct. 1971.
- Bayazeed, A. F., and E. C. Donaldson. 1973. Subsurface disposal of pickle liquor. U.S. Bureau of Mines, Report of Investigations 7804, 31 pp.
- Bergonson, R. 1988. Personal communication. Cabot Corporation, Tuscola, IL 61953.
- Berner, R. A. 1975. The role of magnesium in the crystal growth of calcite and aragonite from sea water. *Geochimica et Cosmochimica Acta*, v. 39, p. 489-504.
- Bohn, H. L., B. L. McNeal, and G. A. O'Connor. 1979. *Soil Chemistry*. John Wiley and Sons, New York, NY, 329 pp.
- Brower, R. D., I. G. Krapac, B. R. Hensel, A. P. Visocky, G. R. Peyton, J. S. Nealon, and M. Guthrie. 1988. Evaluation of current underground injection of industrial waste in Illinois. Final Report HWRIC RR008, Hazardous Waste Research and Information Center, Savoy, IL 61874.
- Chou, S. F. J., and R. A. Griffin. 1983. Soil, clay, and caustic soda effects on solubility, sorption, and mobility of hexachlorocyclopentadiene. *Environmental Geology Notes* 104, Illinois State Geological Survey, Champaign, IL 61820, 54 pp.
- Crowe, A. S., and F. J. Longstaffe. 1987. Extension of geochemical modelling techniques to brines: coupling of the Pitzer equation to PHREEQE, in *Solving ground water problems with models*. The Association of Groundwater Scientists and Engineers, Denver, CO, 10-12 Feb. 1987.
- Donaldson, E. C., and R. T. Johansen. 1973. History of a two-well industrial-waste disposal system, in *Second International Symposium on Underground Waste Management and Artificial Recharge*, v. 1, p. 603-621.
- Goolsby, D. A. 1972. Geochemical effects and movement of injected industrial waste in a limestone aquifer, in T. D. Cook (ed.), *Underground waste management and environmental implications*. American Association of Petroleum Geologists, Memoir 18, p. 355-368.
- Gordon, W., and J. Bloom. 1984. Deeper problems: limits to underground injection as a hazardous waste disposal method. Natural Resources Defense Council, New York, NY.
- Hassett, J. J., and J. J. Jurinak. 1971. Effect of  $Mg^{2+}$  ion on the solubility of solid carbonates. *Soil Science Society of America Proceedings*, v. 35, p. 403-406.
- Headlee, A. J. W. 1950. Interactions between interstitial and injected water, in *Secondary Recovery of Oil in the United States*. American Petroleum Institute, NY, p. 240-245.
- Hower, W. F., R. M. Lasater, and R. G. Mihram. 1972. Compatibility of injection fluids with reservoir components, in T. D. Cook (ed.), *Underground waste management and environmental implications*. American Association of Petroleum Geologists, Memoir 18, p. 287-293.
- Jenne, E. A. 1988. Personal communication. Battelle Pacific Northwest Laboratories, Richland, WA 99352.
- Kamath, K., and M. Salazar. 1986. The role of the critical temperature of carbon dioxide on the behavior of wells injecting hydrochloric acid into carbonate formations, in *International symposium of subsurface injection of liquid wastes*. Underground Injection Practices Council, New Orleans, LA, 3-5 Mar. 1986.
- Kharaka, Y. K., and I. Barnes. 1973. SOLMNEQ: Solution-mineral equilibrium computations. U.S. Geological Survey. National Technical Information Service, PB 215 899, 81 pp.



- LaMoreaux, P. E., and J. Y. Smith. 1985. Waste injection present status and viability. Environmental Institute for Waste Management Studies, University of Alabama, Open File Report, 23 pp.
- Lindberg, R. D., and D. D. Runnells. 1984. Ground water redox reactions: an analysis of equilibrium state applied to Eh measurements and geochemical modeling. *Science*, v. 225, p. 925-927.
- Mehnert, E., C. R. Gendron, and R. D. Brower. 1988. Investigation of the hydraulic effects of deep-well injection of industrial wastes. Final Report. Hazardous Waste Research and Information Center, Illinois (in review).
- Meents, W. F., A. H. Bell, O. W. Rees, and W. G. Tilbury. 1952. Illinois oil-field brines. Illinois State Geological Survey, Illinois Petroleum No. 66, 38 pp.
- Nordstrom, D. K., and J. W. Ball. 1984. Chemical models, computer programs and metal complexation in natural waters, in Kramer, C. J. M., and J. C. Duinker (eds.), *Complexation of trace metals in natural waters*. Martinus Nijhoff/Dr. W. Junk, The Hague, The Netherlands, p. 149-165.
- Nordstrom, D. K., E. A. Jenne, and J. W. Ball. 1979. Redox equilibria of iron in acid mine waters, in Jenne, E. A. (ed.), *Chemical modeling in aqueous systems*. American Chemical Society Symposium Series 93, p. 41-79.
- Ostroff, A. G. 1965. *Introduction to oil field water technology*. Prentice-Hall Inc., Englewood Cliffs, N.J.
- Panagiotopoulos, A. Z., and R. C. Reid. 1986. Deep-well injection of aqueous hydrochloric acid, in *International symposium on subsurface injection of liquid wastes*. Underground Injection Practices Council, New Orleans, LA, 3-5 Mar. 1986.
- Plummer, L. N., B. F. Jones, and A. H. Truesdell. 1976. WATEQF--a FORTRAN IV version of WATEQ, a computer program for calculating chemical equilibrium of natural waters. U.S. Geological Survey--Water Resources Investigations 76-13, 61 pp.
- Ponnamperuma, F. N. 1972. The chemistry of submerged soils. *Advances in Agronomy*, v. 24, p. 29-96.
- Ramette, R. W. 1984. Solution calorimetry in the advanced laboratory. *Journal of Chemical Education*, v. 61, p. 76-77.
- Roedder, E. 1959. Problems in the disposal of acid aluminum nitrate high-level radioactive waste solutions by injection into deep-lying permeable formations. U.S. Geological Survey Bulletin 1088, 65 pp.
- Russell, S. J., and S. M. Rimmer. 1979. Analysis of mineral matter in coal, coal gasification ash, and liquefaction residues by scanning electron microscopy and x-ray diffraction, in Karr, C. (ed.), *Analytical methods for coal and coal products*. Academic Press, New York, NY, v. 3, p. 133-162.
- Scrivner, N. C., K. E. Bennett, R. A. Pease, A. Kopatsis, S. J. Sanders, D. M. Clark, and M. Rafal. 1986. Chemical fate of injected wastes, in *International symposium on subsurface injection of liquid wastes*. Underground Injection Practices Council, New Orleans, LA, 3-5 Mar 1986.
- Skirrow, G. 1975. The dissolved gases-carbon dioxide, in Riley, J. P., and G. Skirrow (eds.), *Chemical Oceanography*, v. 2. Academic Press Inc., London, UK, chapt. 9, p. 1-192.
- Skoog, D. A., and D. M. West. 1976. *Fundamentals of analytical chemistry* (3rd ed.). Holt, Rinehart, and Winston, New York, NY, 804 pp.
- Stumm, W. and J. J. Morgan. 1981. *Aquatic chemistry*. John Wiley and Sons, New York, NY, 780 pp.
- Sullivan, P., M. Essington, R. Poulsen, J. Bowen, J. McKay, and R. Donovan. 1986. Modeling the geochemistry of hazardous waste injection. Report by Western Research Institute, Laramie, WY 82071, 90 pp.
- Truesdell, A. H., and B. F. Jones. 1974. WATEQ, a computer program for calculating chemical equilibria of natural waters. *Journal of Research*, U.S. Geological Survey, v. 2, p. 233-248.
- U.S. Environmental Protection Agency. 1988. Underground injection control program; final rule. *Federal Register*, v. 53, p. 28118-28157.

- U.S. Environmental Protection Agency. 1987. Underground injection control program; proposed rule. Federal Register, v. 52, p. 32446-32476.
- U.S. Environmental Protection Agency. 1980. Hazardous waste management: rules and regulations. Federal Register, v. 45, p. 33110-33112.
- Van Everdingen, R. O., and R. A. Freeze. 1971. Subsurface disposal of waste in Canada. Department of the Environment, Inland Waters Branch, Ottawa, Ontario, Technical Bulletin No. 49, 64 pp.
- Warner, D. L. 1965. Deep-well injection of liquid waste: a review of existing knowledge and an evaluation of research needs: U.S. Department of Health, Education, and Welfare, Public Health Service Publication No. 999-WP-21, 55 pp.
- Warner, D. L., and J. H. Lehr. 1977. An introduction to the technology of subsurface waste water injection: U.S. Environmental Protection Agency, EPA-600/2-77-240, 319 pp.
- Willman, H. B., E. Atherton, T. C. Buschbach, C. Collinson, J. C. Frye, M. E. Hopkins, J. A. Lineback, and J. A. Simon. 1975. Handbook of Illinois Stratigraphy. Bulletin 95, 261 pp.
- Wood, W. W. 1976. Guidelines for collection and field analysis of groundwater samples for selected unstable constituents. U.S. Geological Survey, Techniques of Water-Resources Investigations, chapt. D-2, 24 pp.
- ZoBell, C. E. 1946. Studies on redox potential of marine sediments. American Association of Petroleum Geologists Bulletin, v. 30, p. 477-513.

## APPENDIX A GLOSSARY

<b>carbonate</b>	mineral containing the carbonate ion ( $\text{CO}_3^{2-}$ ) in combination with metal cation(s) such as calcite ( $\text{CaCO}_3$ ) or dolomite ( $\text{CaMg}(\text{CO}_3)_2$ ).
<b>exsolution (gas)</b>	separation of a gas phase from a liquid phase; degassing.
<b>formation brine</b>	subsurface waters present in rock strata that contain a high content of dissolved salts.
<b>hazardous waste</b>	hazardous-waste classification criteria are complex and have been divided into six categories: (1) ignitable, (2) reactive, (3) infectious, (4) corrosive, (5) radioactive, and (6) toxic. Hazardous in this report was applied to solutions having a pH less than 2 or greater than 12.5 as specified by the U.S. EPA (1980).
<b>joule</b>	unit of energy as heat; 1 joule is equal to 0.239 calories.
<b>°K</b>	degrees Kelvin or absolute temperature; based on thermodynamics; related to Fahrenheit as $\frac{9}{5} (^\circ\text{K} - 273.15) + 32 = ^\circ\text{F}$
<b>MPa</b>	megapascals; 106 pascals; unit of pressure; 1 MPa is equal to 145.1 pounds per square inch.
<b>phase</b>	homogeneous, physically distinct portion of matter.
<b>van't Hoff equation</b>	relationship often used to estimate an equilibrium constant for a chemical reaction at a given temperature within a narrow temperature range using

$$\ln (K_{T_i}/K_T) = \frac{-\Delta H}{R} \left( \frac{1}{T} - \frac{1}{T_i} \right)$$

where  $K_{T_i}$  is the equilibrium constant at  $T_i$  (temperature);  $K_T$  is the equilibrium constant at temperature  $T$ ,  $\Delta H$  is the enthalpy of the reaction, and  $R$  is the gas constant.



## **APPENDIX B LABORATORY PROCEDURE FOR CONDUCTING BATCH INTERACTION STUDIES**

### **SUMMARY OF METHOD**

No standardized laboratory procedures are available in the literature for assessing geochemical interactions in deep-well systems. The few publications that address geochemical interactions pertaining to deep-well injection do not present detailed experimental procedures.

One of the products of this project was a first-generation procedure to conduct batch-type interaction studies. This procedure was designed for conducting batch experiments at various pressures and temperatures in a low-oxygen atmosphere. Both gas and aqueous samples can be collected. The procedure is presented as a basis for conducting future studies involving chemical interactions of deep-well systems. The expected variation inherent to this procedure is unknown.

### **LABORATORY EQUIPMENT**

#### **Pressure Vessels**

**Parr 600-mL, 4500 series stirred reactor or equivalent** The size of vessel may vary; however, a minimum head space requirement for a given size vessel must be determined using the maximum allowable water loading formula as given by the manufacturer. Figure B1 is a schematic representation of the pressure vessel. Minor modifications of the vessels were performed to improve overall performance.

**Vessel modification** We observed that on occasion fine particles (from the disaggregated sample) would be expelled from the gas-release port during the purging step via the liquid sample delivery tube. The tube originally reached down into the solid sample at the bottom of the vessel. Hence, the delivery tube was shortened by approximately 3 cm.

The stirring impellers were raised along the stirring shaft to prevent particle abrasion and to protect the stirring motors from fatigue. To accommodate collection of gas samples, a fitting containing a syringe needle and septum was added to the gas-release valve of each pressure vessel. A Swagelok® Quick-Connect fitting was added to the gas-inlet-liquid injection system to allow ease of pressurization.

**Chemical compatibility of vessels** It must be noted that the pressure vessels were not chemically inert, and were subject to attack by the waste liquids used in this study. Consequently, the appearance of certain chemical constituents in solution had to be carefully considered. The average composition of the two types of vessels used was known (table B1). The data summarized in table B1 indicated that most of the artifact concentrations were low. However, because of the acidic nature of the acidic waste-Mt. Simon system, the acid-resistant (Hastelloy B-2) vessels were used exclusively with this combination. This application yielded relatively high concentrations of Fe, Ni, and Mo. When the Mt. Simon Sandstone was mixed with the acidic waste in Nalgene bottles, Fe was from the sandstone, but at lower levels than those associated with the pressure vessels (fig. B2). Analysis of available data indicated that the acidic waste-Mt. Simon system was the most severe case in terms of solute artifacts. Hence, this problem was a limitation for acidic systems when using Hastelloy B-2. Iron chemistry was not discussed in this paper because of the uncertain nature of the source of iron in solution. It was found that coating the impellers with a liquid plastic reduced solution artifacts associated with the bombs. Another possibility would be Teflon liners. Titanium pressure vessels are commercially available and would probably be more suitable for acidic systems. However, they are extremely expensive and were beyond the budget for this project.

**Cleaning procedures** After each experiment, the pressure vessels were opened, and the remaining slurry was discarded. The stirring impellers were removed from the shafts. The reactor cylinders, impellers, and all other surfaces that were in contact with the liquids were

rinsed with tap water, then set into a cleaning bath containing 3 percent to 6 percent  $\text{HNO}_3$  for 20 minutes. The components were then rinsed with deionized water four times, and allowed to air dry. All ports on the reactor heads were opened and flushed with deionized water for 20 minutes followed by acetone. Excess moisture was blown from the ports and associated surfaces with compressed nitrogen.

### Water Baths

Constant-temperature water baths capable of maintaining temperatures between 20 and 60°C ( $\pm 2$ ) were used to control solution temperatures within the vessels. The water baths may be eliminated if vessel-temperature controllers are purchased.

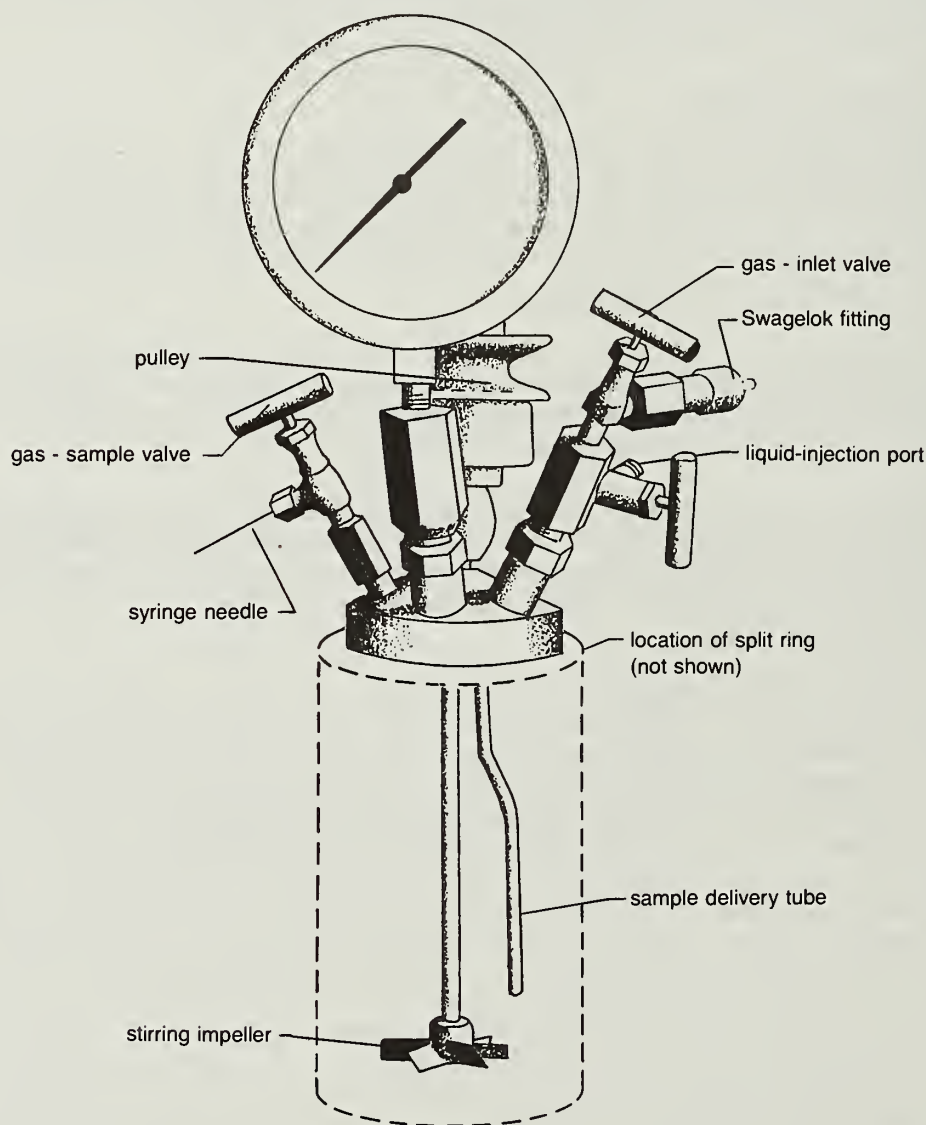


**Figure B1** Parr pressure vessel with modifications.

**Table B1** Composition of the pressure vessels and occurrence of solute artifacts

Metal	Stainless steel T316 (%)	Blank <sup>a</sup> (mg/L)	Hastelloy (%)	Blank <sup>b</sup> (mg/L)	Cabot waste <sup>c</sup> (mg/L)
Co	--	<0.03	--	--	0.13
Cr	17	0.23	1	0.10	<0.02
Fe	65	<0.02	2	82.0	24.9
Mo	2.5	0.10	28	12.3	<0.02
Mn	2.0	<0.01	1	2.13	1.51
Ni	12	0.03	66	58.5	<0.03
Si	1.0	1.08	--	--	7.23

<sup>a</sup>3 M NaCl, pH 12.7 solution was mixed in a pressure vessel at 328°K-11.7 MPa for 16 days.

<sup>b</sup>Values shown are the differences between solutions generated by the pressure vessels and Nalgene plastic bottles at 298°K-100 kPa by mixing the acidic Cabot waste with Mt. Simon for 15 days. For example, the concentration of iron in the solution using a Hastelloy pressure vessel was 182 mg/L. When the sandstone was mixed with the acidic waste in a plastic bottle, the solution contained 100 mg/L of iron. A "blank" was approximated as 182-100 = 82 mg/L (see figure B2).

<sup>c</sup>Composition of the waste before mixing (from table 1).

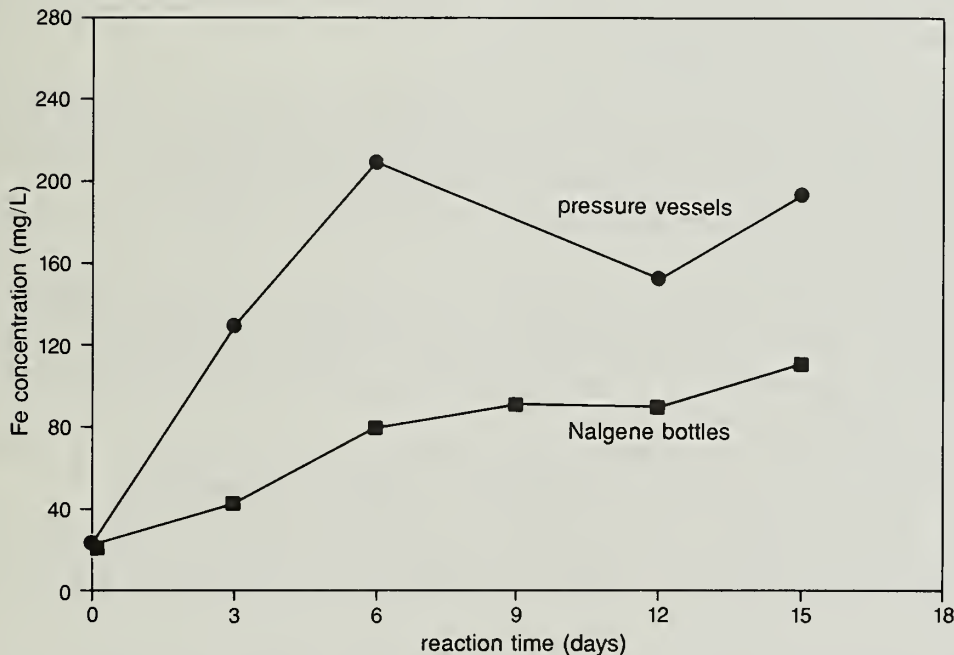


**Figure B2** Solution iron concentration in the acidic liquid waste when mixed with the Mt. Simon Sandstone at 298°K-0.1 MPa in the Hastelloy pressure vessels and in Nalgene plastic bottles.



### Gas Collection Containers

Glass serum vials (Pierce No. 12995) having a volume of 125 mL and fitted with a Teflon-lined septum and aluminum seals were found to make excellent gas collection containers. Also, Vacutainer blood collection tubes (100 × 13 mm) were also used to collect gas samples. Both types of gas collection containers were evacuated for 20 minutes at 64 mmHg of vacuum before use. These containers were found to leak after about 2 days; thus, analysis should be done as soon as possible.

### PREPARATION OF FORMATION SAMPLES

The formation samples were spread out on a flat surface. Since the formation samples were in the form of cores, initial crushing with a jaw crusher was used to facilitate drying. The samples were allowed to air dry until they were in equilibrium with the moisture content of the room atmosphere. (If samples are to be kept anaerobic, they can be processed in a glove box filled with an oxygen-free inert gas to prevent oxidation.) The samples were reduced to pass a 2-mm screen sieve using a Roll jaw crusher. The selection of this size fraction was arbitrary. The sieved material was mixed until homogeneous using a riffle splitter. The moisture content of the air-dried sample was determined using ASTM-D2216, Laboratory Determination of Moisture Content of Soils Method. The mass of sample required for study was corrected for moisture such that the oven-dry weight of sample was used in all calculations.

### PROCEDURE

- 1 Place the disaggregated sample into the pressure vessel. A 1:4 solid-to-liquid ratio (wt/vol) was selected on the basis of preliminary methods testing. It was found that a lower ratio, i.e., more mass, could not be efficiently mixed without fatiguing the stirring motors and/or without the suspensions binding the stirring impellers.
- 2 Assemble the pressure vessel, tightening the split-ring bolts in a diagonal pattern.
- 3 Evacuate the pressure vessel through the liquid-injection port for 20 minutes at 64 mmHg of vacuum.
- 4 Purge the vessel with nitrogen at 6 L/min for 20 minutes with all valves open, then close the valves, leaving a slight positive pressure.
- 5 Repeat steps 3 and 4 twice, each for 10 minutes.
- 6 Collect a blank gas sample (to define the atmospheric composition of the vessel before the liquid is added) by bayoneting the Teflon-lined septum on the glass serum vial onto the syringe needle on the gas-release valve. Open the valve for 15 seconds.
- 7 Collect two replicate gas samples using the Vacutainer blood collection tubes, opening the valve for 1 to 2 minutes.
- 8 Fill a 250-mL glass syringe with the liquid waste and attach it to the liquid-injection port. The tip of the syringe is fitted with a short (15 mm) piece of Tygon tubing, which serves as a leak-proof junction between the syringe and valve. Open the valve and discharge the solution into the vessel while (if needed) occasionally opening the gas-sample valve to allow for gas displacement.
- 9 Pressurize the vessel by attaching a high-pressure hose to the Swagelok fitting. Pressurize the vessels using a nitrogen tank equipped with a high-pressure regulator.
- 10 Place the pressure vessel into the water bath, and attach a belt to the pulley on top of the vessel (to facilitate mixing). The stirring motors are controlled by timers to allow the motors to cool periodically. Stir the mixture in each vessel at 120 rpm for 30 minutes every 3 hours.
- 11 At the end of the experiment, connect a high-pressure 6.9 MPa in-line filter with a 0.45- $\mu$ m filter membrane to the liquid-injection port. Open the valve slightly to allow the internal pressure to push the liquid out via the delivery tube. Where non-pressurized investigations are desired, pour the solution from the vessel into a suitable filtration apparatus using a 0.45- $\mu$ m filter membrane. (To avoid oxidation, pouring may require a glove box filled with an oxygen-free inert gas.)

- 12 Discharge the filtered solution into a glass container that is immediately capped with no head space to retard degassing. Determine the pH and Eh of this solution by quickly removing the stopper and replacing it with another stopper with holes to insert the electrodes.
- 13 Collect additional samples for instrumental and laboratory analysis as quickly as possible using the same method.
- 14 Degas the pressure vessels to approximately 170 Pa.
- 15 Collect three gas samples to define the post-contact composition of the head space using steps 6 and 7.

**APPENDIX C GEOLOGIC DESCRIPTIONS OF CORE INTERVALS  
SAMPLED FOR THIS PROJECT**

**Table C1** Description of the Potosi Dolomite

Description	Thickness (meters)	Bottom (meters)
Dolomite, sandy, light gray and pink mottled, fine and coarse, glauconitic, vuggy; green clay infiltration	1.5	375.5
Dolomite, partly sandy, light brownish gray to light gray, fine; considerable green clay infiltration at top; few bands of dolomite, pinkish brown, coarse; scattered pea-size vugs, some quartz-lined	6.1	381.6
Dolomite, sandy, light gray, fine as matrix; fragments of dolomite, pinkish brown, coarse; some green clay infiltration; sand disseminated throughout and concentrated in zones; core badly mixed	2.3	383.9
Sandstone, medium, numerous coarse grains; green clay infiltration	0.1	384.0
Dolomite, gray, slightly brownish, fine, vuggy; green clay and tripolitic chert infiltration	0.9	384.9
Dolomite, partly sandy, brownish gray, compact, hard, few scattered vugs lined with drusy quartz	0.4	385.3
Dolomite, light brownish gray, fine; some glauconite and green clay along irregular bedding planes	0.3	385.6
Dolomite, gray, fine to medium, slightly glauconitic, highly vuggy, vugs lined with coarse dolomite crystals; green clay along irregular contacts and disseminated through dolomite in small patches	0.6	386.2
Dolomite, brownish gray, fine, crystalline, vuggy	0.3	386.5
Dolomite, grayish brown, very fine	0.1	386.6
Dolomite, brownish gray, fine compact, sub-oolitic, vuggy, highly broken; some green clay infiltration	0.6	387.2
Dolomite, light brownish gray, very fine to fine, slightly glauconitic	1.4	388.6
Core loss	0.9	389.5
Dolomite, grayish brown, fine slightly glauconitic	0.4	389.9
Dolomite, gray, fine, vuggy, some drusy quartz and coarse dolomite in vugs	1.3	391.2
Dolomite, brownish gray, fine compact, scattered vugs as above	0.5	391.7



Table C1 *continued*

Description	Thickness (meters)	Bottom (meters)
Dolomite, brownish gray, very fine compact	0.3	392.0
Dolomite, brownish gray, very fine to fine, sub-oolitic vuggy, slightly glauconitic	0.7	392.7
Dolomite, brownish gray, extra fine, dense	0.2	392.9
Dolomite, brownish gray, fine to medium, slightly glauconitic, vuggy, sub-oolitic in lower 0.1 m	1.0	393.9
Dolomite, dark brown, fine to medium, crystalline	0.1	393.9
Dolomite, light brownish gray, fine; hard small pebbles like underlying rock in basal 2 cm	0.1	394.0
Dolomite, very silty, greenish white, extra fine, slightly glauconitic, hard, compact	0.5	394.5
Dolomite, light gray, very fine, finely glauconitic, scattered vugs	0.3	394.8
Dolomite, brownish gray, fine, finely glauconitic, large syngenetic crystals of calcite up to 1 cm	0.3	395.1
Dolomite, gray, fine to medium, few vugs, almost no glauconite, massive and hard; some green shale and stylolitic partings	1.4	396.5
Dolomite, light gray, fine to medium crystalline, massive, hard, slightly glauconitic, vuggy, coarse dolomite in vugs; few zones appear to have medium crystals in sparse aphanitic ground mass	3.5	400.0
Dolomite, as above, massive, very vuggy	2.9	402.9
Dolomite, gray, fine to medium crystalline, vuggy, massive	1.5	404.4
Dolomite, as above, but vugs larger and more abundant	2.7	407.1
Dolomite, as above; medium gray, fine to medium, faintly sub-oolitic, vuggy, faint brownish color below 408.4, finely laminated in some zones, little drusy quartz in vugs	6.4	413.5
Dolomite, grayish brown, fine, crystalline, vuggy; irregular bands and blebs of tripolitic chert	0.6	414.1
Dolomite, light grayish brown, white mottled, fine, crystalline, vuggy, massive; irregular masses of tripolitic chert	5.8	419.9

**Table C2** Description of the Proviso Siltstone of the Eau Claire Formation

Description	Thickness (meters)	Bottom (meters)
Interbedded: 1) Sandstone, silty, dolomitic, very fine scattered coarse, pyritic; 2) Shale, silty, sandy, greenish gray, fissile, numerous brachiopod fragments	0.3	572.7
Shale, sandy in part, greenish gray, fissile, fossiliferous	0.9	573.6
Dolomite, silty, argillaceous, very fine, laminated greenish gray and brownish gray	0.6	574.2
Shale, silty, green, fissile, fossiliferous; interlaminated with dolomite, silty, grayish brown, very fine, fossiliferous; some interbedded sandstone in basal 2 cm, very dolomitic, fine, gray, slightly glauconitic	1.8	576.0
Glauconite rock, medium to granule, rounded, polished, pyritic, cemented by fossiliferous dolomite	0.15	76.1
Shale, silty, dolomitic, greenish gray, slightly glauconitic, hard; little interlaminated siltstone, dolomitic, gray; at base is a bed of glauconite rock as above	0.3	576.4
Shale, silty, dolomitic, greenish gray, micaceous, some interlaminated siltstone, dolomitic, grayish brown, fossiliferous; much core loss	4.4	580.8
Siltstone, dolomitic, gray; some interbedded shale, silty, dark gray, slightly greenish, hard	0.5	581.3
Conglomerate, matrix of dolomite, silty, red, fine, full of coarse white crinoid fragments; pebbles of dolomite, very silty, green, very fine	0.1	581.4
Interbedded and interlaminated: 1) Siltstone, dolomitic, brownish gray, hard, micaceous (80%); 2) Shale, silty, dark greenish gray (20%); below 581.9 siltstone has pale yellowish organic cast; solid shale 586.4-586.7	6.0	587.4
Siltstone, and shale, as above, very micaceous	1.5	588.9
Shale, silty, dark greenish gray, fissile	0.4	589.3
Finely interlaminated siltstone, gray, and shale, dark gray; contains pebbles of siltstone, yellowish orange	0.2	589.5
Interlaminated and interbedded: 1) Siltstone, slightly dolomitic, grayish orange (80%); 2) Shale, silty, dark greenish gray, fissile (20%)	2.3	591.8

Table C2 *continued*

Description	Thickness (meters)	Bottom (meters)
Siltstone and shale, as above glauconite and some fossil material finely scattered and concentrated in thin laminae	2.4	594.2
Shale, silty, black, micaceous, fissile, some laminations, slightly lighter colored	0.3	594.5
Interbedded and interlaminated siltstone and shale as above	0.5	595.0
Siltstone, slightly dolomitic, grayish orange, finely glauconitic, micaceous; interlaminated with shale, black, micaceous, massive, thick bedded	1.2	596.2
Shale, silty, black, micaceous, fissile	0.3	596.5
Siltstone, slightly dolomitic to dolomitic toward base, coarse, micaceous, finely glauconitic, scattered fossil fragments; interlaminated and interbedded with 20% shale, dark greenish gray, silty, micaceous, fissile; shale more prominent below 604.4	10.1	606.6
Siltstone, slightly dolomitic, brownish gray, micaceous, finely glauconitic, thick bedded, massive	1.1	607.7
Interbedded and interlaminated: 1) Siltstone, gray to grayish orange, micaceous, finely glauconitic, few small brachiopods, (80%); 2) Shale, black to dark green, micaceous, fissile (20%)	5.0	612.7
Shale, silty, dark chocolate brown micaceous, brittle, rather fissile	0.2	612.9
Interbedded and interlaminated: 1) Siltstone, slightly dolomitic, grayish orange, micaceous, slightly glauconitic; 2) Siltstone, dolomitic, gray, coarse to finely sandy, very micaceous, glauconitic; 3) Shale, dark greenish gray, micaceous, fossiliferous	1.1	614.0



**Table C3** Description of the Mt. Simon Sandstone

Description	Thickness (meters)	Top (meters)
Sandstone, medium to coarse grained, dark to light gray, interbedded clasts, some cross bedding	0.3	435.9
Sandstone, medium to fine grained, brownish-white, faint black mottling	1.2	436.2
Sandstone, fine grained, white with red hues	0.5	437.4
Sandstone, medium grained, grayish white, black streaks, pyrite-shale films, bedded	0.5	437.9
Sandstone, medium grained, tan, relatively clean	0.2	438.4
Sandstone, medium to coarse grained, tan, black streaks	1.4	438.6
Sandstone, fine to medium grained, tan, black streaks, irregular bedding	0.9	440.0
Sandstone, medium grained, light tan-white with black mottling	0.2	440.9
Sandstone, medium grained, tan, cross bedded, faint black mottling	1.4	441.1
Sandstone, fine grained tannish-white with red hues	0.6	442.5
Sandstone, medium to coarse grained, tannish-white, red hues and gray streaks	0.9	443.1
Sandstone, medium grained, tan with prominent red and black bands	0.3	444.0
Sandstone, fine grained, red	0.3	444.3
Sandstone, medium grained, tan with red hues, cross bedded	1.8	444.6
Sandstone, medium to coarse grained, brown with black streaks	0.6	446.4
Sandstone, medium grained, tan	0.6	447.0
Sandstone, medium grained, tan with faint red hues	0.2	447.6
Sandstone, medium grained, red with black bands, minor cross bedding	0.5	447.8
Sandstone, medium grained, tan, cross bedded	1.2	448.3
Sandstone, medium to coarse grained, tan to brown	not measured	449.5

## APPENDIX D APPLICATION OF ION CHROMATOGRAPHY TO DERIVE OXIDATION-REDUCTION POTENTIALS

The measurement of the oxidation-reduction potential (Eh) of a solution is usually conducted with a platinum electrode or a saturated calomel electrode. It is well known that such measurements are difficult to duplicate and that readings of a sample solution with two identical electrodes may vary by as much as 50 mV depending on the stability of the solution, electrode, and the skill of the analyst (references cited in Nordstrom et al., 1979). Moreover, it is not always certain when the electrode has equilibrated with a solution; often the reading may slowly drift, and not stabilize on a constant value.

In this project, Eh measurements were determined with a platinum electrode, and referenced to a temperature-corrected ZoBell solution. It was observed that when the solutions were collected from the in-line filter attached to the pressure vessels, discarded aliquots would oxidize (table D1). As the Eh readings increased, the solutions would often become colored and opaque, particularly the solutions subjected to the higher temperatures and pressures. The pH of the same solutions remained constant. It was difficult to determine when the electrode was equilibrated, and at what point oxidation was becoming significant. All redox measurements given in this report were obtained within two minutes of sample collection. During this interval, the electrode readings rapidly decreased from ambient conditions, reached a minimum, then slowly increased. A concomitant coloration of the solution was observed during this latter step. Also, the solutions began to degas as evidenced by the formation of bubbles on the sides of the container.

**Table D1** Oxidation-reduction potential measurements as a function of time

Eh (mV)	Time since collection (min)
-68	1
-11	16
+34	24
+112	33
+172	42
Potosi-Cabot system at 313°K-6 MPa; data not corrected to a ZoBell solution	

To derive more reliable Eh data for interpretations, some investigators have attempted to measure the specific activities of the known dominant redox couple, and calculate an Eh via the Nernst equation,

$$Eh = Eh^{\circ} - \frac{RT}{\eta F} \ln \frac{\Pi_i(ox)^{m_i}}{\Pi_j(red)^{m_j}}$$

where Eh is the redox potential of the system,  $Eh^{\circ}$  is the standard electrode potential at temperature T, R is the gas constant, F is Faraday's constant, h is the number of electrons transferred in the reaction, ox and red are the thermodynamic activities of the oxidized and reduced constituents, and m is the stoichiometric coefficient of the reaction.

As summarized by Nordstrom et al. (1979), some investigators have found good agreement between the measured Eh and a dominant redox couple, while others regard Eh measurements

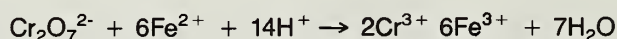
as only a qualitative indication of the redox potential. In a study by Lindberg and Runnells (1984), multiple redox couples yielded calculated potentials that spanned over a range of 1000 mV. In this project, ion chromatography (IC) was applied to determine the concentrations of  $\text{Fe}^{2+}$  and  $\text{Fe}^{3+}$  in order to derive Eh values to compare with the electrode-based observations.

The specific analytical methods used for the IC determinations are given in the methods section. The application of ion chromatography to determine iron couples is a relatively new concept and apparently not widely tested. No literature or documentation is available on analytical techniques or limitations. The solutions for Fe analyses by IC were collected from the in-line filter, and immediately acidified to a pH less than 1.8 with sulfuric acid.

Several problems were encountered during this phase of the study. It was found that acidified Fe(II) standards were partially converted to Fe(III) after injection into the IC column-detector system. Depending on the initial concentration of Fe(II), between 5 and 20 percent of the iron was oxidized. At low concentrations (0.5 mg  $\text{Fe}^{2+}$ /L), nearly all of the iron was converted to Fe(III). The PDCA eluant was degassed and purged with nitrogen, but oxidation problems persisted. Problems were also encountered due to the limited linear range of the ion chromatograph (~10 mg  $\text{Fe}^{2+}$ /L). The samples had to be diluted thereby introducing another step for potential oxidation to  $\text{Fe}^{3+}$ . Because of the inability to measure  $\text{Fe}^{2+}$  accurately, emphasis was given to Fe(III) determinations. It was found that Fe(III) measurements were not reproducible to better than a 15 percent coefficient of variation, but improvement was gained by matching the matrix of the standards with the samples (CV = 7 percent). As a next step in the study, the concentration of Fe(II) was estimated by subtracting Fe(III) from the total amount of iron in solution.

The activities of  $\text{Fe}^{2+}$  and  $\text{Fe}^{3+}$  were then calculated after species distribution and temperature correction by WATEQ2. The program calculated an Eh value for each solution using the Nernst equation. These calculated Eh potentials were in poor agreement with the electrode-based measurements (fig. D1). The IC data suggested that the systems were very oxidized, and that the iron couple was dominated by  $\text{Fe}^{3+}$ . Given the oxygen-poor conditions of the pressure vessels, the data were suspect. Moreover, it was known that Fe(II) standards tended to be partially oxidized; hence, it was concluded that the Fe(III) concentrations in the samples as determined by IC were erroneous.

As an alternative method, ferrous iron was determined by titrating the solutions with dichromate using a combination platinum electrode (see Skoog and West, 1976). This method more correctly determines the concentrations of all reduced species. It is assumed that the oxidation of  $\text{Fe}^{2+}$  is the dominant reaction consuming  $\text{Cr}_2\text{O}_7^{2-}$  in the presence of acid,



The values for  $\text{Fe}^{2+}$  concentration by titration were in poor agreement with those obtained by ion chromatography (fig. D2). The titrimetric data indicated that  $\text{Fe}^{2+}$  dominated the iron couple, which was in qualitative agreement with the Eh values. Under reduced conditions,  $\text{Fe}^{2+}$  would be the most stable form of ionic iron. These data further indicated that the IC did not yield reliable data.

The concentration of  $\text{Fe}^{3+}$  in the sample solutions was estimated by subtracting the titrimetric  $\text{Fe}^{2+}$  from total iron. Redox potentials were then calculated as before using WATEQ2. At 298°K, the calculated (via titration) potentials were in fair agreement with measured values, although calculated potentials were somewhat higher. Nordstrom et al. (1979) also applied WATEQ2 to calculate Eh potentials, and found that calculated values tended to suggest more oxidized conditions than those implied by electrode measurement. The activities used in these types of calculations were not directly measured, but were predicted by equilibrium modeling. Nordstrom



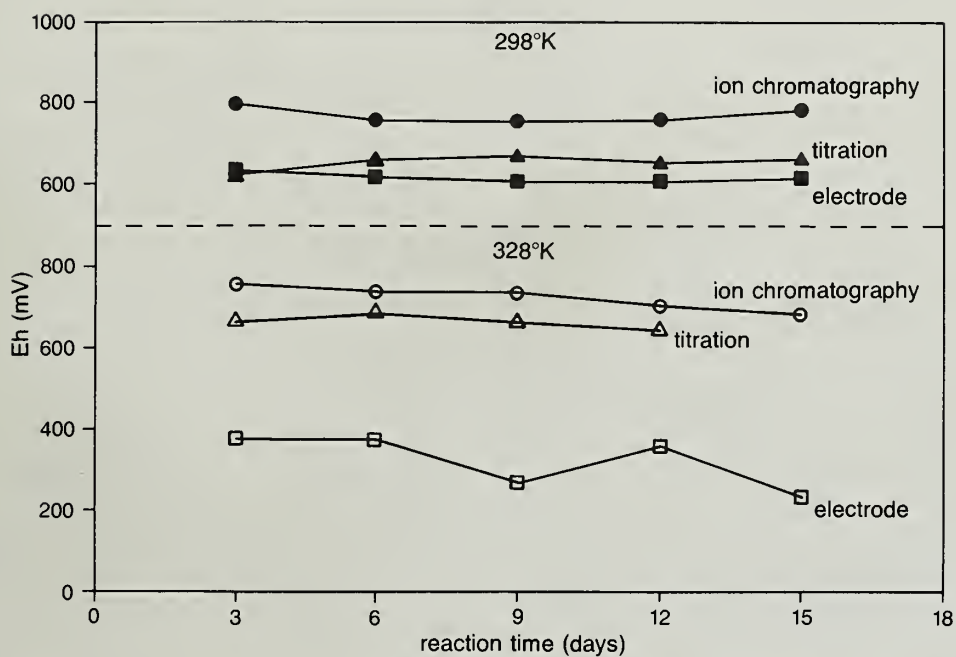


**Figure D1** Distribution of oxidation-reduction potentials as a function of time for the Mt. Simon-acidic waste mixture derived by ion chromatography, dichromate titration, and platinum electrode.

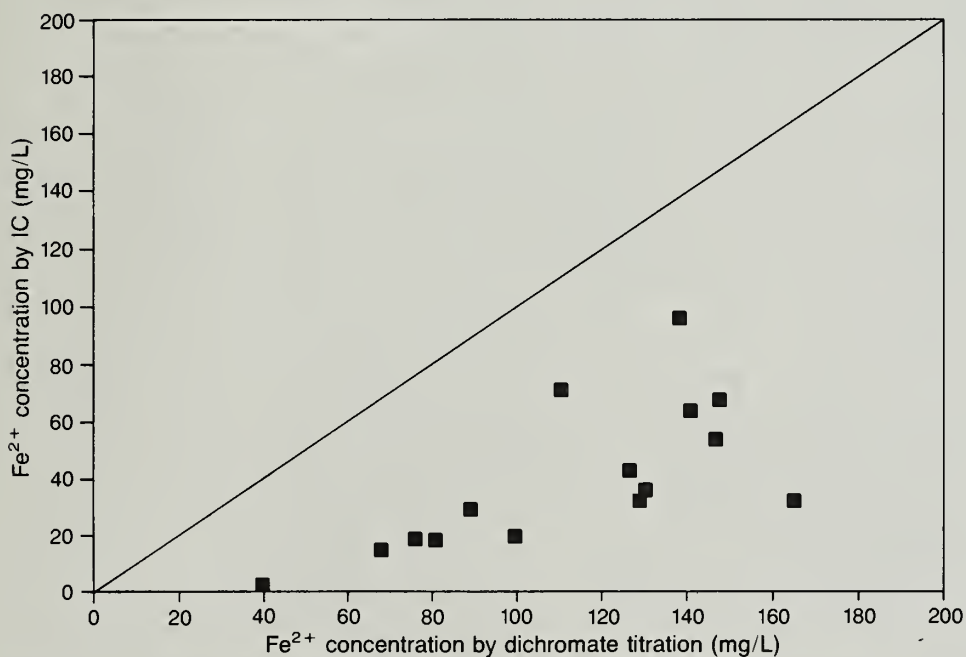


**Figure D2** Agreement between  $\text{Fe}^{2+}$  determinations derived from dichromate titration and ion chromatography.

et al. (1979) speculated that Fe(III) complexes are quite strong, and some complexes were not considered by WATEQ2 due to a lack of reliable thermodynamic data.

At the higher temperatures and pressures, the Eh potentials derived from the titrations were in poor agreement with electrode-based potentials (fig. D1). The lack of agreement was not resolved. Inspection of equation D1 indicates that under reducing conditions, the concentration of  $\text{Fe}^{3+}$  may be very low, requiring very accurate analytical determinations. Moreover, even minor oxidation can have a major impact on the calculated potential. Due to the short interval of this study, further research was not possible. It should be noted that when a redox electrode is immersed into a solution, the observed reading may reflect the summation of different individual redox couples, and this combined potential may differ greatly from that of any known potential (Bohn et al., 1979). The potential of a platinum electrode in a redox mixture may be a poorly defined average of the potentials of all redox couples present. The contribution of each couple to the observed measurement is an unknown function of its concentration. For example, nitrate stabilizes potentials at 0.2 to 0.4 V and prevents the formation of  $\text{Fe}^{2+}$  in soils (Ponnamperuma, 1972). In summary, the redox potentials given in this report had only qualitative value. The data presented cast serious doubt on the ability of ion chromatography to yield reliable iron-couple data without considerably more research. Because of the greater need for analytical sensitivity for  $\text{Fe}^{3+}$  in reduced systems (i.e., fig. D1), further methods development is required to make measuring iron couples a viable alternative for deriving redox potentials as opposed to electrode measurements, especially in complex solutions.













HECKMAN  
BINDERY INC.



**JUN 97**

Bound-To-Please® N. MANCHESTER,  
INDIANA 46962



